

ragonal transition at the equilibrium state occurs at about 550 °C. Here we have shown that under CH<sub>4</sub> atmosphere the onset temperature is lowered by at least 150 °C. This result is consistent with the assumption that the out-diffusion rate of oxygen in the YBaCuO compound is limited by a surface barrier of 1.7 eV, which is involved in the surface diffusion of O<sup>-</sup> species and the further formation and desorption of O<sub>2</sub>.<sup>13</sup> In the presence of methane this surface barrier is lowered as a result of the strong

chemical interaction between O<sup>-</sup> surface species and CH<sub>4</sub> molecules of the gas phase.

New experiments are being conducted in our laboratory in order to determine the catalytic properties of the YBaCuO superconductor in the selective oxidation of methane to C<sub>2</sub> hydrocarbons in the presence of free molecular oxygen.

Registry No. CH<sub>4</sub>, 74-82-8; YBa<sub>2</sub>Cu<sub>3</sub>O<sub>7</sub>, 109064-29-1.

## FEATURE ARTICLE

### Excited States, Electron-Transfer Reactions, and Intermediates in Bacterial Photosynthetic Reaction Centers

Steven G. Boxer,\* Richard A. Goldstein, David J. Lockhart, Thomas R. Middendorf, and Larry Takiff

Department of Chemistry, Stanford University, Stanford, California 94305 (Received: April 4, 1989)

The three-dimensional structure of a photosynthetic reaction center has recently been obtained at atomic resolution using X-ray crystallography by Deisenhofer, Epp, Miki, Huber, and Michel [*J. Mol. Biol.* **1984**, *180*, 385-398; *Nature* **1985**, *318*, 618-624]. This breakthrough provides the fundamental structural information needed to understand the mechanisms of the initial energy- and electron-transfer steps in photosynthesis. The structure reveals the distances among the reactive bacteriochlorophylls and quinones as well as the location of all nearby solvent molecules, the amino acids of the reaction center protein. Thus, the reaction center provides a complex but well-defined solid-state reactive system for the study of fundamental physical and chemical processes with implications and applications well beyond this specific system. We review recent studies of the reaction intermediates and mechanism of electron transfer in which the energetics and reaction dynamics have been perturbed with external electric and magnetic fields. These approaches complement picosecond transient absorption spectroscopy and theoretical treatments of the problem. Electron-transfer mechanisms which have been proposed are reviewed critically in light of the available data, and electron transfer in the reaction center is compared with electron transfer in other biological and nonbiological systems.

#### Introduction

The initial charge separation and energy storage steps in photosynthesis take place in a membrane bound, chlorophyll-protein complex called the photosynthetic reaction center (RC). In this article, we will focus on the initial photophysical and photochemical processes that take place in RCs from photosynthetic bacteria. The three-dimensional structure of the RC from two species of purple non-sulfur bacteria has been determined to atomic resolution during the past several years<sup>1-6</sup> as shown in Figure 1. The breakthrough was the crystallization of the protein complex by Michel,<sup>7</sup> followed by solution of the X-ray crystal structure by Deisenhofer et al.<sup>1</sup> Although a great deal of spectroscopic and kinetic data<sup>8</sup> had been obtained before the crystal structure was solved, the availability of the atomic coordinates of all the reactive components and their solvent (the RC protein) prior to charge separation has stimulated great interest in un-

derstanding the underlying physics of the RC function.

At the outset, it is worth noting a few of the features of these initial events that have stimulated the interest of so many physical chemists. It is probably safe to say that no other system undergoing long-distance electron transfer has been studied in so much detail both experimentally and theoretically. In addition, this system has provided the inspiration for many ingenious model systems. The primary electron donor, a strongly interacting but not covalently connected pair of bacteriochlorophylls called P, is electronically excited either directly or by highly efficient energy transfer from other pigments within the RC or the adjacent antenna complex. The lowest energy singlet electronic excited state of P, <sup>1</sup>P, decays within a few picoseconds by electron transfer to produce the charge-separated intermediate, P<sup>+</sup>H<sup>-</sup>, where H is a monomeric bacteriopheophytin (Figure 1).<sup>9-14</sup> Not only is the reaction very fast, but it is also only weakly dependent on temperature, actually speeding up as the temperature is decreased.<sup>9,12</sup> Since the donor and acceptor are separated by about 10 Å (edge-to-edge), this is a remarkably rapid long-distance elec-

(1) Deisenhofer, J.; Epp, O.; Miki, K.; Huber, R.; Michel, H. *J. Mol. Biol.* **1984**, *180*, 385-398.

(2) Deisenhofer, J.; Epp, O.; Miki, K.; Huber, R.; Michel, H. *Nature* **1985**, *318*, 618-624.

(3) Michel, H.; Epp, O.; Deisenhofer, J. *EMBO J.* **1986**, *5*, 2445-2451.

(4) Allen, J. P.; Feher, G.; Yeates, T. O.; Komiyama, H.; Rees, D. C. *Proc. Natl. Acad. Sci. U.S.A.* **1987**, *84*, 5730-5734.

(5) Allen, J. P.; Feher, G.; Yeates, T. O.; Komiyama, H.; Rees, D. C. *Proc. Natl. Acad. Sci. U.S.A.* **1987**, *84*, 6162-6166.

(6) Chang, C. H.; Tiede, D.; Tang, J.; Smith, U.; Norris, J. *FEBS Lett.* **1986**, *205*, 82-86.

(7) Michel, H. *J. Mol. Biol.* **1982**, *158*, 567-572.

(8) Kirmaier, C.; Holten, D. *Photosynth. Res.* **1987**, *13*, 225-260.

(9) Woodbury, N. W.; Becker, M.; Middendorf, D.; Parson, W. W. *Biochemistry* **1985**, *24*, 7516-7521.

(10) Martin, J. L.; Breton, J.; Hoff, A. J.; Migus, A.; Antonetti, A. *Proc. Natl. Acad. Sci. U.S.A.* **1986**, *83*, 957-961.

(11) Breton, J.; Martin, J. L.; Migus, A.; Antonetti, A.; Orszag, A. *Proc. Natl. Acad. Sci. U.S.A.* **1986**, *83*, 5121-5125.

(12) Fleming, G. R.; Martin, J. L.; Breton, J. *Nature* **1988**, *333*, 190.

(13) Kirmaier, C.; Holten, D. *FEBS Lett.* **1988**, *239*, 211-218.

(14) Breton, J.; Martin, J. L.; Fleming, G. R.; Lambry, J. C. *Biochemistry* **1988**, *27*, 8276-8284.

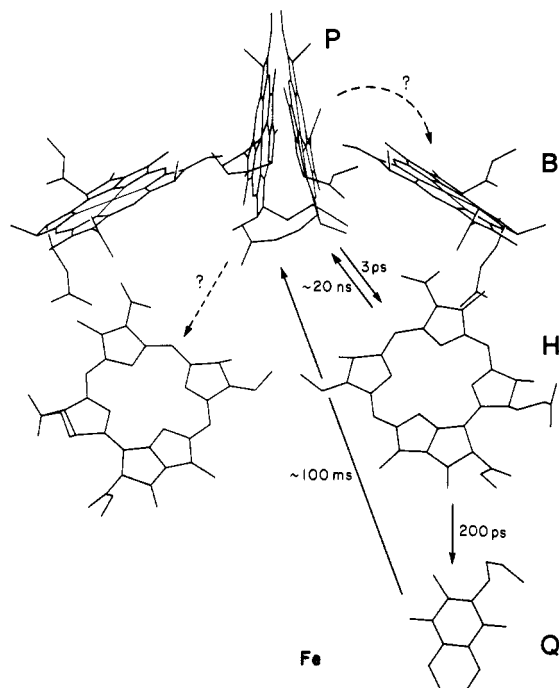


**Figure 1.** Arrangement of the chromophores in the reaction center of *Rps. viridis*.<sup>1</sup> P is the special pair electron donor; B is the monomeric bacteriochlorophyll *b* on the L-side (right side as drawn) of the RC; H is the monomeric bacteriopheophytin *a* on the L-side; Q is the quinone ( $Q_A$ ). The distances among these components are listed in Table I. The room-temperature rates are shown (cf. Figure 3B). The dashed arrows are electron transfers which have not been directly observed. The approximate  $C_2$  axis of symmetry runs roughly vertically from the geometric center of P to the Fe atom.

tron-transfer reaction. The role of intervening chromophores and protein residues in facilitating this reaction is a subject of intense interest. From  $H^+$  the electron transfers to a quinone, labeled  $Q_A$ , in about 100 ps to form  $P^+HQ_A^-$ ; the electron then moves in about 100  $\mu s$  to a second quinone, labeled  $Q_B$ , to form  $P^+HQ_AQ_B^-$ .<sup>8</sup> The electron-transfer kinetics at room temperature are summarized in Figure 1, along with the back electron transfer rates determined by using RCs with subsequent electron acceptors either removed or reduced. The forward rates are several orders of magnitude faster than the recombination rates, ensuring a high quantum efficiency of charge separation.

Because the chromophores involved in these reactions are neutral, closed-shell molecules in their ground state, the intermediate states have two characteristics. First, charge is separated over a considerable distance, so the states have large electric dipole moments; second, a radical pair is formed. The large electric dipole moment makes it possible to manipulate the relative energies of these intermediates and consequently the reaction dynamics with external electric fields. The presence of unpaired electrons in the radical pair allows the reaction dynamics to be altered with external magnetic fields. Because of the wide range of experimental and theoretical tools that have been used to study RCs, much is known about their structure and function. Therefore, the electron-transfer reactions in the photosynthetic RC offer an exceptional opportunity to test and refine theories of electron transfer with specific applications to long-distance electron transfer in proteins, to develop new methods to study electron transfer, and to establish which parameters are important for efficient artificial photosynthesis.

In the following, we review some details of the properties of RCs. We then focus on three experimental issues that have been the primary concerns of our laboratory: the nature of the lowest energy singlet electronic excited state of P, the identity of the initial electron acceptor, and the energetics of the initial charge separation step. Obviously, there are other important experimental and theoretical issues which have occupied the attention of other laboratories but which will not be discussed in detail; up-to-date

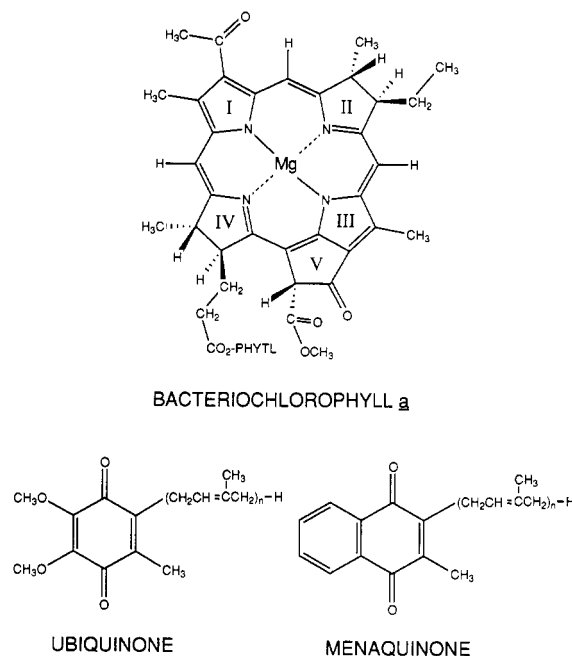


**Figure 2.** Structure of bacteriochlorophyll *a*, ubiquinone, and menaquinone. In the bacteriopheophytins, two protons replace the central Mg ion. Bacteriochlorophyll *b* has an ethylidene in place of an ethyl group in ring II.

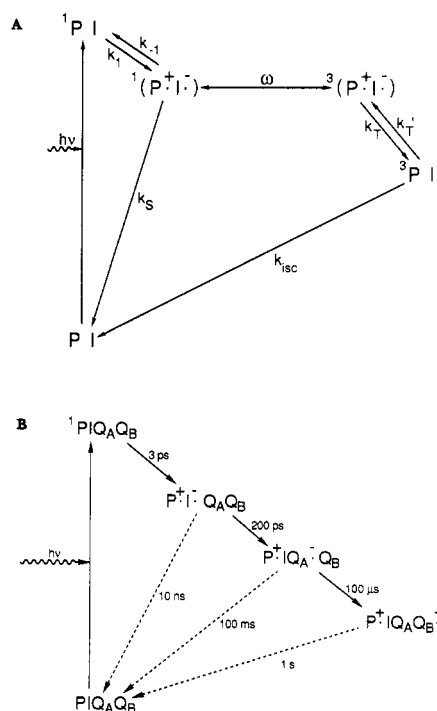


**Figure 3.** Reaction schemes without (A) and with (B)  $Q_A$  (see Figure 13 for energetics).

summaries can be found in recent monographs.<sup>15</sup>

**Properties of the Reaction Center.** The RC is the smallest isolable unit which performs the initial charge separation steps of photosynthesis.<sup>16</sup> By far the best studied RCs are those isolated from two species of purple bacteria: *Rhodobacter sphaeroides* and *Rhodospseudomonas viridis*. The arrangement of the reactive components of the RC from *Rps. viridis* is shown in Figure 1;<sup>1</sup>

(15) *The Photosynthetic Bacterial Reaction Center—Structure and Dynamics*; Breton, J., Vermeglio, A., Eds.; Plenum: New York, 1988. *Perspectives in Photosynthesis*; Jortner, J., Pullman, B., Eds.; Elsevier Press: Amsterdam, 1989.

(16) Feher, G.; Okamura, M. Y. In *The Photosynthetic Bacteria*; Clayton, R. K., Sistrom, W. R., Eds.; Plenum Press: New York, 1978; pp 349–386.

**TABLE I: Distances (in Å) among Chromophores in the *Rps. viridis* RC Structure<sup>a,b</sup>**

	P <sub>L</sub>	B <sub>L</sub>	H <sub>L</sub>	Q <sub>A</sub>	Fe	P <sub>M</sub>	B <sub>M</sub>	H <sub>M</sub>
P <sub>L</sub>		5.5	9.5	22.4	23.7	2.5	5.7	12.2
B <sub>L</sub>	10.4		4.8	19.5	25.2	5.4	14.5	17.8
H <sub>L</sub>	16.5	10.2		9.7	15.5	11.7	18.1	16.9
Q <sub>A</sub>	28.2	23.4	14.3		6.8	22.8	28.2	19.8
Fe	27.8	26.1	18.0	8.6		23.6	26.6	16.2
P <sub>M</sub>	7.0	12.6	19.0	28.6	27.8		6.1	9.8
B <sub>M</sub>	13.0	21.4	24.3	30.9	26.9	10.9		5.7
H <sub>M</sub>	19.7	24.4	23.4	24.1	18.7	17.1	10.9	

<sup>a</sup> The values above the diagonal are edge-to-edge distances, and those below the diagonal are center-to-center distances. <sup>b</sup> Taken from ref 116. The reader accustomed to small molecule structural data is cautioned that the *Rps. viridis* X-ray structure is at 2.3-Å resolution with an *R* factor of 0.23; thus, typical uncertainties in distance are 0.2 Å or more. Theoretical calculations or interpretations of experimental results which are sensitive to distance changes of several tenths of an angstrom are likely not to be definitive.

the arrangement of the chromophores in *Rb. sphaeroides* is very similar.<sup>4-6</sup> The chromophores shown in Figure 1 are encased in two hydrophobic proteins, designated L and M, whose combined molecular weight is approximately 60 kDa. As isolated, both species of RC contain a third polypeptide which is not associated with the chromophores and, in the case of *Rb. sphaeroides* RCs, can be removed without affecting function.<sup>16</sup> The chromophores in *Rb. sphaeroides* RCs are a-type bacteriochlorophylls; they are b-type in *Rps. viridis* (Figure 2). Both quinones are ubiquinone in *Rb. sphaeroides*; Q<sub>A</sub> is menaquinone in *Rps. viridis*. Both species contain a cytochrome which donates an electron to reduce P<sup>+</sup>. In *Rb. sphaeroides* the cytochrome is loosely bound and does not co-crystallize with the RC; the cytochrome in *Rps. viridis* is firmly bound, and its structure is also now known (not included in Figure 1).<sup>1</sup> The quinones and cytochromes are extremely important to photosynthetic function, but their role will not be discussed in the following (see ref 15). RCs have one molecule of bound carotenoid which has recently been located in the crystal structures.<sup>17,18</sup> A carotenoidless mutant of *Rb. sphaeroides*, *R-26*, has been the most extensively characterized spectroscopically.<sup>16</sup> All RCs have a non-heme iron located between the quinones whose function is not certain.<sup>19</sup> The distances between the components in *Rps. viridis* are given in Table I.

A remarkable feature of the RC structure is the presence of an approximate C<sub>2</sub> axis of local symmetry roughly along the line connecting the geometric center of dimeric P and the iron atom. Rotation about this axis by 180° exchanges the positions of the two BChls comprising P, the two monomeric BChls (often designated B), the monomeric bacteriopheophytins (often labeled H; BPheo is BChl in which two protons replace the central Mg ion), and the quinones. The chromophores on the right-hand side of the RC as drawn in Figure 1 are called the L-side chromophores, P<sub>L</sub>, B<sub>L</sub>, and H<sub>L</sub>, while the chromophores on the left side are called the M-side chromophores, P<sub>M</sub>, B<sub>M</sub>, and H<sub>M</sub>, corresponding roughly to the protein subunit which comprises the dominant fraction of the binding site of the chromophore. The symmetry at the level of the reactive chromophores extends even to the transmembrane α-helices comprising the principal secondary structure of the proteins.<sup>2</sup> The symmetry is broken by slight differences in the distances among the chromophores along the L and M branches (Table I), by differences in the orientations of some chromophore ring substituents, and by differences in the amino acid side chains on the two proteins. Electron transfer appears to occur exclusively along the L branch;<sup>8,20</sup> thus, the symmetry is also broken at the level of function. The evidence for this unidirectionality of electron flow has been discussed in detail by several investigators,<sup>8,20</sup> and understanding its origin at the molecular level has become a major challenge for theorists and experimentalists.

## Mechanism of Charge Separation

**Photochemical Hole-Burning Spectroscopy.** Prior to the recent subpicosecond measurements of the initial charge separation dynamics,<sup>9-14</sup> the time constant for the initial electron transfer could not be resolved below about 10 ps.<sup>8</sup> We decided that photochemical hole-burning spectroscopy might offer an alternative approach to characterizing this initial step. It has been known for many years that the absorption band corresponding to electronic excitation from the ground state to the first excited singlet state of P is bleached following broad-band excitation of the RC because P<sup>+</sup> has negligible absorption where P absorbs.<sup>16</sup> This bleach lasts for tens of milliseconds at cryogenic temperatures until P<sup>+</sup>Q<sub>A</sub><sup>-</sup> decays by charge recombination, as shown in Figure 1. (At low temperature, the electron is not transferred from Q<sub>A</sub> to Q<sub>B</sub>.) By observing the line width of the absorption bleach following narrow-bandwidth laser excitation within the P absorption band, it should be possible to separate the homogeneous broadening of the P absorption band due to the lifetime of <sup>1</sup>P from any inhomogeneous broadening due to a distribution of interactions between P and its environment. Because the lifetime of <sup>1</sup>P is very short, the lifetime-limited homogeneous line width (determined by the uncertainty principle) has to be larger than about 1 cm<sup>-1</sup>.

To our surprise narrow-bandwidth excitation at various wavelengths within the absorption band of P leads to a bleaching of nearly the entire absorption band. We specifically looked for narrow features in the hole-burning spectrum at the excitation wavelength (resolution 0.5 cm<sup>-1</sup>) both for *Rb. sphaeroides*<sup>21</sup> and *Rps. viridis*.<sup>22</sup> RCs embedded in poly(vinyl alcohol) matrices, but we have no evidence for a narrow hole feature in any of our samples within the signal-to-noise at the burn wavelengths used (see below). The simplest interpretation of this result is to ascribe the approximately 400-cm<sup>-1</sup> hole width to an ultrashort excited-state lifetime (about 20 fs). This interpretation ignores vibrational structure within the absorption band; an excited-state lifetime of 200 fs would be sufficient to smear out any structure in the hole if the vibronic spacing were typical of molecules of this type.<sup>23,24</sup> The notion that the broad holes should be interpreted in terms of an ultrafast (tens of femtoseconds) electronic decay of <sup>1</sup>P into an intermediate state has been championed by Wiersma and co-workers, who performed hole-burning and accumulated photon-echo experiments on these systems independently of our work.<sup>25,26</sup> Although it is difficult to conceive of a process occurring with such a fast rate at 1.5 K, charge separation within dimeric P<sup>21,22,25,26</sup> and excimer formation<sup>21,22</sup> were suggested possibilities. The RC fluorescence quantum yield measured more than 20 years ago<sup>27</sup> predicts a <sup>1</sup>P lifetime on the order of a few picoseconds

(17) Deisenhofer, J.; Michel, H. In *The Photosynthetic Bacterial Reaction Center—Structure and Dynamics*; Breton, J., Vermeglio, A., Eds.; Plenum: New York, 1988; pp 1-5.

(18) Yeates, T. O.; Komiya, H.; Chirino, A.; Rees, D. C.; Allen, J. P.; Feher, G. *Proc. Natl. Acad. Sci. U.S.A.* **1988**, *85*, 7993-7997.

(19) Debus, R. J.; Feher, G.; Okamura, M. Y. *Biochemistry* **1985**, *24*, 2488-2500; **1986**, *25*, 2276-2287.

(20) Michel-Beyerle, M. E.; Plato, M.; Deisenhofer, J.; Michel, H.; Bixon, M.; Jortner, J. *Biochem. Biophys. Acta* **1988**, *932*, 52-70.

(21) Boxer, S. G.; Lockhart, D. J.; Middendorf, T. R. *Chem. Phys. Lett.* **1986**, *123*, 476-482.

(22) Boxer, S. G.; Middendorf, T. R.; Lockhart, D. J. *FEBS Lett.* **1986**, *200*, 237-241.

(23) Renge, I.; Mäuring, K.; Avarmaa, R. *J. Lumin.* **1987**, *37*, 207-214.

(24) Platenkamp, R. J.; Den Blanken, H. J.; Hoff, A. J. *Chem. Phys. Lett.* **1980**, *76*, 35-41.

(25) Meech, S. R.; Hoff, A. J.; Wiersma, D. A. *Chem. Phys. Lett.* **1985**, *121*, 287-292.

(26) Meech, S. R.; Hoff, A. J.; Wiersma, D. A. *Proc. Natl. Acad. Sci. U.S.A.* **1986**, *83*, 9464-9468.

(assuming a reasonable radiative lifetime of several nanoseconds), consistent with recent subpicosecond time-resolved absorption and stimulated emission experiments.<sup>9-14</sup> The stimulated emission data in particular show that the decay of the population of the emitting state parallels the growth of the state  $P^{+}H^{-}$ . However, these experiments cannot rule out the possibility that the initially formed excited state decays very rapidly (subpicoseconds) to the emitting state (which lives for picoseconds) because of the time resolution and the uncertain spectral identification of such states. The results of experiments that measure the effect of an electric field on the fluorescence from RCs<sup>28</sup> discussed below argue against such a mechanism.

We also proposed the alternative hypothesis that the holes are broad and the zero-phonon line is very weak not because of a rapid electronic or vibrational decay process but because the excited-state manifold of  $^1P$  is substantially different from that of the ground state, either in its equilibrium nuclear configuration or in the density of states and vibrational level spacing or both. In this case the Franck-Condon factor for the 0-0 transition is very small, and the electronic transition is primarily to a higher energy region of the excited-state manifold which is congested due to low-frequency vibrational and/or phonon modes<sup>22</sup> (i.e., the levels in the relevant region of the excited-state manifold are not just unresolved, but unresolvable). Two possible mechanisms are that  $^1P$  has substantial dipolar character, due, for example, to mixing with charge-transfer states of the dimer, or that the macrocycles comprising the dimer move following excitation, as in excimer formation.<sup>22</sup> Note that although the physical mechanisms described here and in the previous paragraph are closely related, the first model postulates decay of the initially formed  $^1P$  state on a subpicosecond time scale into a different electronic state prior to formation of  $P^{+}H^{-}$ , while the alternative model postulates that the excited state of  $^1P$  is itself quite different from the ground state. In the first model, the zero-phonon hole is expected to be broad because of the postulated subpicosecond electronic decay and relatively intense; in the second model, the zero-phonon hole is expected to be very weak with a width that reflects the excited-state lifetime due to the  $^1P \rightarrow P^{+}H^{-}$  reaction, accompanied by a broad background bleaching.

Several investigators have published more detailed theoretical treatments of the hole-burning experiments related to the physical models outlined above. Small and co-workers postulated very strong linear electron-phonon coupling in the RC;<sup>29,30</sup> this could most readily be explained if  $^1P$  were very polar and interacted strongly with the protein matrix. However, the amino acids in the vicinity of P are rather nonpolar,<sup>2</sup> and there is evidence (see below) that  $^1P$  is only moderately polar. Later, Small and co-workers obtained hole-burning spectra of *Rps. viridis* RCs in glycerol/water matrices which exhibit a very small, narrow feature at the burn wavelength and some unresolved structure in the dominant broad background hole.<sup>31</sup> The small narrow feature was interpreted as the residual zero-phonon hole, while the broader substructure was interpreted as partly due to a progression in a moderately low frequency mode ( $\sim 150\text{ cm}^{-1}$ ) and partly due to a new electronic state of P, suggested to be a charge-transfer state. Very recently, spectra for both *Rb. sphaeroides* and *Rps. viridis* RCs in both glycerol/water and poly(vinyl alcohol) (PVA) matrices were obtained by these investigators.<sup>32,33</sup> Although the data are similar to those in ref 31, it was argued that the broader

substructure is due entirely to a progression in the moderately low frequency mode, i.e., that there is no evidence for an underlying electronic state. Furthermore, the line width of the very small zero-phonon hole corresponds roughly to the low-temperature lifetime of  $^1P$  measured by transient absorption spectroscopy.<sup>9,12</sup> If the latter proves to be true, this is strong evidence against an ultrafast electronic decay process occurring on a time scale much faster than the  $^1P \rightarrow P^{+}H^{-}$  electron-transfer reaction. The observation of narrow holes that are exceedingly weak in addition to a much more intense and broad background hole is consistent with the second model described above and agrees qualitatively with the earlier experimental results, while providing potentially valuable additional information.

One of the difficulties in comparing these very recent results with those obtained earlier is that the ground-state absorption spectrum is different, showing a shoulder on the red side of the special pair absorption band. This shoulder depends on the medium and has been observed by others (ref 34 and references therein). The absorption Stark effect, which is very sensitive to underlying structure in the absorption line shape, shows no evidence for this shoulder at 77 K in PVA (see below). Shuvalov and co-workers have recently demonstrated that narrow holes are obtained if  $H^{-}$  accumulates in the sample.<sup>35</sup> Although the data obtained by Small and co-workers in ref 32 and 33 use gated detection, trace amounts of accumulated intermediates ( $H^{-}$  or other intermediates) could complicate the analysis of very weak, narrow features.

Won and Friesner have proposed that the broad holes result from congestion in the excited-state manifold due to strong vibronic coupling between  $^1P$  and a nearly resonant electronic state.<sup>36,37</sup> Although the precise nature of this state was not specified, likely candidates are intramolecular charge-transfer states of the dimer (sometimes called  $P^{+}P^{-}$ ) or intermolecular charge-transfer states such as  $P^{+}B^{-}$ . This model is quite sensitive to the energy of charge-transfer states, and the simulations based on this model are also consistent with the hole-burning data. Further experimental and theoretical work is clearly required to decide among competing models and interpretations. A recurring theme in each of these models is the importance of charge-transfer states; thus, it is natural to consider electric field effect measurements on the RC in order to gain further insight into the dipolar character of RC excited states.

**Stark Effect Measurements on RCs.** The Stark effect has long been used to probe the change in dipole moment associated with optical transitions. Many investigators have used this technique to probe the nature of the ground and excited states of simple aromatic molecules, and extensive reviews are available.<sup>38-40</sup> There are few applications of this method to biological systems, a notable exception being the work of Mathies and Stryer on the retinal chromophore,<sup>41</sup> in which it was demonstrated that there is a very substantial change in the electric dipole moment between the ground and excited state along the long axis of the polyene. DeLeeuw and co-workers presented a Stark effect spectrum for RCs at a meeting several years ago;<sup>42</sup> stimulated by that preliminary result and the hole-burning data, our laboratory<sup>43-45</sup> and

(27) Zankel, K. L.; Reed, D. W.; Clayton, R. K. *Proc. Natl. Acad. Sci. U.S.A.* **1968**, *61*, 1243.

(28) Lockhart, D. J.; Goldstein, R. F.; Boxer, S. G. *J. Chem. Phys.* **1988**, *88*, 1408-1415.

(29) Hayes, J. M.; Small, G. J. *J. Phys. Chem.* **1986**, *90*, 4928.

(30) Hayes, J. M.; Gillie, J. K.; Tang, D.; Small, G. J. *Biochim. Biophys. Acta* **1988**, *932*, 287-305.

(31) Tang, D.; Jankowiak, R.; Gillie, J. K.; Small, G. J.; Tiede, D. M. *J. Phys. Chem.* **1988**, *92*, 4012-4015.

(32) Tang, D.; Johnson, S. G.; Jankowiak, R.; Hayes, J. M.; Small, G. J.; Tiede, D. M. In *Perspectives in Photosynthesis*; Jortner, J., Pullman, B., Eds.; in press.

(33) Johnson, S. G.; Tang, D.; Jankowiak, R.; Hayes, J. M.; Small, G. J.; Tiede, D. M. *J. Phys. Chem.* **1989**, *93*, 5953.

(34) Klevanik, A. V.; Ganago, A. O.; Shkurapov, A. Ya.; Shuvalov, V. A. *FEBS Lett.* **1988**, *237*, 61-64.

(35) Shuvalov, V. A.; Klevanik, A. V.; Ganago, A. O.; Shkurapov, A. Ya.; Gubanov, V. S. *FEBS Lett.* **1988**, *237*, 57-60.

(36) Won, Y.; Friesner, R. A. *Proc. Natl. Acad. Sci. U.S.A.* **1987**, *84*, 5511.

(37) Won, Y.; Friesner, R. A. *J. Phys. Chem.* **1988**, *92*, 2214-2219.

(38) Liptay, W. In *Excited States*; Lim, E. C., Ed.; Academic: New York, 1974; Vol. 1, pp 129-229.

(39) Hochstrasser, R. *Acc. Chem. Res.* **1973**, *6*, 263-269.

(40) Mathies, R. A. Ph.D. Dissertation, Cornell University, 1974.

(41) Mathies, R. A.; Stryer, L. *Proc. Natl. Acad. Sci. U.S.A.* **1976**, *73*, 2169.

(42) DeLeeuw, D.; Malley, M.; Buttermann, G.; Okamura, M. Y.; Feher, G. *Biophys. Soc. Abstr.* **1982**, *37*, 111a.

(43) Lockhart, D. J.; Boxer, S. G. *Biochemistry* **1987**, *26*, 664-668, 2958.

(44) Boxer, S. G.; Lockhart, D. J.; Middendorf, T. R. *Springer Proc. Phys.* **1987**, *20*, 80-90.

(45) Lockhart, D. J.; Boxer, S. G. *Proc. Natl. Acad. Sci. U.S.A.* **1988**, *85*, 107-111.

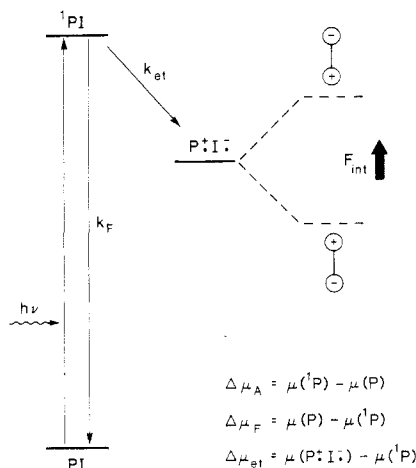


**Figure 4.** Definition of dipole moments of states and difference dipole moments. The solid lines are schematic energy levels in zero electric field (see Figure 13 for actual energetics). For an isotropic immobilized sample in an applied electric field, the energy of the  $P^+I^-$  state increases or decreases depending on the orientation of the  $P^+I^-$  dipole; the largest changes occur for dipoles oriented parallel or antiparallel to the field and are illustrated with the dotted levels. The ground and excited states of P may also have nonzero dipole moments; however, these are likely to be smaller than the  $P^+I^-$  dipole moment and are not shown for simplicity. The intermediate electron acceptor I may be either B or H (cf. Figure 1) as discussed in the text.

several others<sup>46-48</sup> have undertaken more quantitative studies.

The absorption or emission spectrum of a randomly oriented, immobilized sample is broadened in an applied electric field if there is a difference in the permanent electric dipole moment,  $\Delta\mu$ , between the ground and excited state involved in an optical transition. (The labeling of states is illustrated in Figure 4.) In the case that this is the dominant effect, the change in absorption or fluorescence in an electric field,  $\Delta A$  or  $\Delta F$ , is directly proportional to  $|\Delta\mu|^2$ , to the second derivative of the absorption or emission spectrum, and to the square of the electric field felt by the chromophore under consideration,  $F_{int}$ .  $F_{int}$  is different from the applied field  $F_{ext}$  due to the dielectric properties of the material in the vicinity of the chromophore,  $F_{int} = fF_{ext}$ .<sup>117</sup> While the value of the local field correction  $f$  is somewhat uncertain, the differences in the observed values of  $|\Delta\mu_A|$  for different chromophores in the RC are sufficiently large that the main conclusions are not likely to be changed by variations in  $f$ . In addition, the conclusions based on the direction of  $\Delta\mu_A$  are independent of the magnitude of  $f$ .<sup>117</sup>

Since  $\Delta\mu_A$  and  $\Delta\mu_F$  are vector quantities, it is possible to measure the angle (denoted  $\zeta_A$  and  $\zeta_F$  for absorption and fluorescence, respectively) between them and the transition dipole moment of the transition used to probe the effect. The orientation of the transition dipole moment with respect to the molecular axes can be determined independently with considerable precision from single-crystal polarized absorption spectroscopy and emission polarization measurements. Thus, a measurement of  $\zeta$  gives information on the direction of the charge displacement associated with the spectroscopic transition in a molecule-based axis system. Moreover, assuming that  $f$  can be represented by a scalar,<sup>117</sup> the determination of the value of  $\zeta$  does not depend on the local field correction, so we have stressed this observable in our analysis. For the experimental geometry shown in Figure 5, the dependence of  $\Delta A$  on the experimental angle  $\chi$  between the direction of the applied electric field and the electric vector of the probing light is given by the following expression:

$$\Delta A(\chi) \propto 5 + (3 \cos^2 \chi - 1)(3 \cos^2 \zeta_A - 1) \quad (1)$$

(46) Lösche, M.; Feher, G.; Okamura, M. Y. *Proc. Natl. Acad. Sci. U.S.A.* **1987**, *84*, 7537.

(47) Lösche, M.; Feher, G.; Okamura, M. Y. In *The Photosynthetic Bacterial Reaction Center—Structure and Dynamics*; Breton, J., Vermeiglio, A., Eds.; Plenum: New York, 1988; pp 151-164.

(48) Braun, H. P.; Michel-Beyerle, M. E.; Breton, J.; Buchanan, S.; Michel, H. *FEBS Lett.* **1987**, *221*, 221-225.

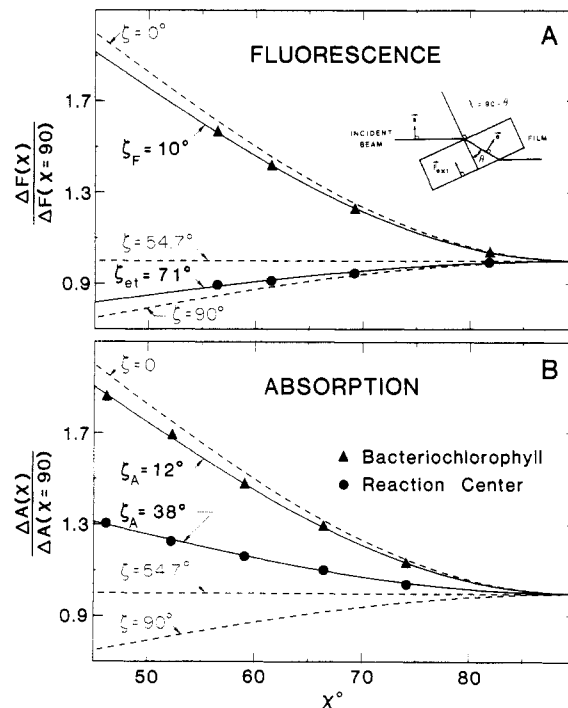


**Figure 5.** (A) Dependence of  $\Delta F(\chi)/\Delta F(\chi=90^\circ)$  on the experimental angle  $\chi$  for quinone-depleted *Rb. sphaeroides* reaction centers (circles) and the dependence of  $\Delta F(\chi)/\Delta F(\chi=90^\circ)$  on  $\chi$  for six-coordinate bacteriochlorophyll *a* in poly(methyl methacrylate) (triangles) along with the best fit of the data for  $\zeta_{et}$  or  $\zeta_F$  using eq 3 or 1, respectively. (B) Dependence of  $\Delta A(\chi)/\Delta A(\chi=90^\circ)$  on the experimental angle  $\chi$  for the special pair  $Q_y$  absorption band of *Rb. sphaeroides* reaction centers. In (A) and (B), plots of  $\Delta F(\chi)/\Delta F(\chi=90^\circ)$  and  $\Delta A(\chi)/\Delta A(\chi=90^\circ)$  vs  $\chi$  calculated from eq 1 for  $\zeta$  equal to  $0^\circ$ ,  $54.7^\circ$ , and  $90^\circ$  are shown (dashed lines) to illustrate the sensitivity of the measurement to this angle.

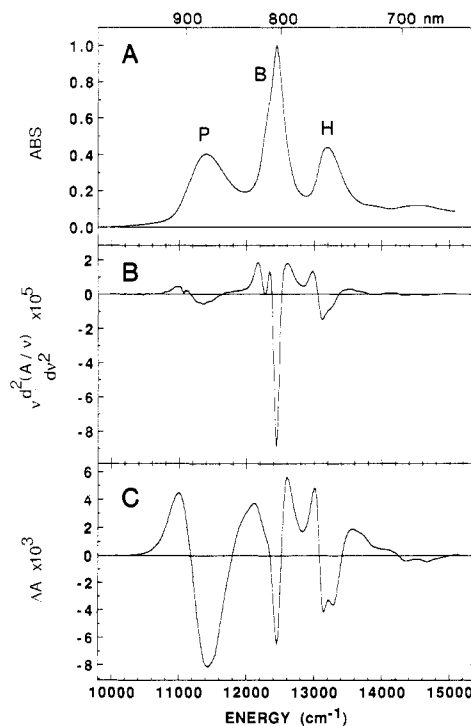


**Figure 6.** Absorption (A), second-derivative (B), and Stark effect (C) for *Rb. sphaeroides* RCs in a PVA film in the  $Q_y$  region at 77 K. The data have been scaled to  $A(802) = 1.0$  and  $F_{ext} = 1.0 \times 10^6$  V/cm.

Along with the data discussed below, Figure 5 shows plots using eq 1 for  $\zeta = 0^\circ$ ,  $54.7^\circ$ , and  $90^\circ$ .

The Stark effect spectrum for *Rb. sphaeroides* RCs in the region of excitation to the lowest singlet electronic excited states

of the chromophores is shown in Figure 6.<sup>43-48</sup> Each feature in the Stark effect spectrum has the approximate shape of the second derivative of the corresponding absorption band, demonstrating that the change in dipole moment is sufficiently large to dominate effects due to the change in polarizability (which would give a Stark line shape that is the first derivative of absorption; see below) or changes in the oscillator strength (which would give a Stark line shape that is the zeroth derivative of absorption). As shown, the effect of the field on the special pair  $Q_Y$  transition at 870 nm is greater than that on the bands corresponding to excitation of the monomers B (802 nm) or H (760 nm).  $|\Delta\mu_A|$  for the B monomers is nearly identical with the value found for pure BChl *a* in a simple polymer matrix,<sup>45</sup> while  $|\Delta\mu_A|$  for the special pair is about 3-4 times larger (about 7 D/f at 77 K). In addition, the value of  $\zeta_A$  for the special pair is considerably larger than for isolated monomeric chromophores (Figure 5). A further more subtle observation is that the special pair absorption band is homogeneous with respect to  $\zeta_A$ , providing no indication of underlying structure or significant variation in the electronic nature of the states across the band.

While the value of  $|\Delta\mu_A|$  is too small for  $^1P$  to be a pure charge-transfer state involving full charge separation between the monomeric constituents of P or between P and the nearby monomeric chromophores, the Stark effect data indicate that the excited state of the special pair is substantially more dipolar than that of a monomeric chromophore.<sup>118</sup> This is not a general feature of dimers as demonstrated by studies of synthetic chlorophyllide dimer model compounds.<sup>49</sup> One can obtain a crude estimate of the energy of a pure charge-transfer state for dimeric P ( $P^{+}P^{-}$ ) from the reduction potential of monomeric neutral and cationic bacteriochlorophyll. This energy is near to the energy of the first singlet excited state of the dimer, but a precise estimate is difficult without a detailed understanding of the stabilization of this hypothetical state by the protein, an issue that has been discussed in detail by Warshel and Parson.<sup>50,51</sup> Although there are features in the Stark effect spectrum whose origin is not obvious by comparison with the various derivatives of the absorption spectrum, we have not unequivocally identified new bands in the Stark effect spectrum or observed strong enhancement of transitions to higher excited states as has been observed in the Stark effect spectra of crystalline anthracene,<sup>52</sup> tetracene,<sup>53</sup> pentacene,<sup>53</sup> phthalocyanine,<sup>54</sup> and some chlorophyll derivatives.<sup>55</sup> Unlike these simpler crystalline materials, there are several different types of chromophores in the RC that interact. Thus, in addition to admixture of  $P^{+}P^{-}$  character into  $^1P$ , admixture of  $P^{+}B^{-}$  and  $P^{+}H^{-}$  states may also be important. Since the Stark effect for special pair transitions in the  $Q_x$  and Soret regions is not unusually large,<sup>45</sup> we conclude from a simple perturbation theory argument that the important pure charge-transfer states lie closer in energy to the lowest electronic state ( $Q_Y$  transition) than to these higher energy states.

Scherer and Fischer<sup>56</sup> and Parson (personal communication) have noted that significant electric-field-induced changes in the mixing between states would be evident as a first-derivative contribution to the absorption Stark effect spectrum (an electric-field-induced shift of the absorption band). This is true unless the states involved are nearly degenerate in zero field or if there are two symmetry-related states (dipoles in opposite directions) of different energies which are mixed with a third state whose energy is intermediate between the other two. An example of the latter situation could arise in the RC if the energy of the excitonic

state of P were in between those of the intradimer charge-transfer states  $P_L^{+}P_M^{-}$  and  $P_M^{+}P_L^{-}$  (which could have different energies because of differing degrees of stabilization by the protein environment). In these special cases, the electric-field-induced change in the mixing can result in line shape contributions other than the first derivative, as will be discussed below. Such field-induced changes would not be surprising since the energies of dipolar states such as  $P^{+}P^{-}$  and  $P^{+}B^{-}$  can be changed by many hundreds of wavenumbers in an electric field of  $10^6$  V/cm ( $10^6$  meV/Å). In addition, depending on the zero-field energy difference between  $^1P$  and the relevant charge-transfer states, the dependence of  $\Delta A$  on electric field strength could deviate from quadratic at high fields, and the angle  $\zeta_A$  could be field dependent.  $\zeta_A$  is found to be independent of field up to  $F_{\text{ext}} = 4.6 \times 10^5$  V/cm (the highest field at which it has been measured), and the Stark effect line shape is independent of field and contains very little of a first-derivative component for fields up to  $F_{\text{ext}} = 1 \times 10^6$  V/cm. Furthermore, the magnitude of  $\Delta A$  increases as the square of the field strength between about  $7 \times 10^4$  and  $1 \times 10^6$  V/cm. The important implications of these observations will be discussed later.

The measured value of  $\zeta_A$  can provide additional information about the initially excited state. However, because  $\Delta\mu_A$  is a difference dipole moment and the magnitude and direction of the ground-state dipole moment are not known, definitive statements cannot be made at this time. Also, the observed angle  $\zeta_A = 38 \pm 2^\circ$  only defines cones around the transition dipole moment direction. Nonetheless, it is striking that  $\zeta_A$  for the special pair is the same for *Rb. sphaeroides* and *Rps. viridis* RCs,<sup>45,46</sup> even though the values of  $\zeta_A$  for the individual monomers comprising the dimers (BChl *a* and *b*, respectively) are quite different (Figure 5)<sup>45</sup> and that  $\zeta_A$  for the special pair is considerably larger than for the monomers. The common feature of the two RCs is their structure, suggesting that  $\zeta_A$  for the special pair reflects a common structural feature. Taking the direction of the transition moment obtained from single-crystal polarized absorption measurements on *Rps. viridis*,<sup>57</sup> we can estimate hypothetical values of  $\zeta_A$  assuming the dipolar character of  $^1P$  is determined by mixing with the state  $P^{+}P^{-}$  (the direction of this dipole is taken simply as the line drawn between the centers of the two monomers in the special pair,  $\zeta_A \sim 31^\circ$ ) or  $P^{+}B^{-}$  (the direction of this dipole is taken as a line drawn between the geometric center of the special pair and the center of B,  $\zeta_A \sim 46^\circ$ ). Because the special pair itself has nearly  $C_2$  symmetry, but not inversion symmetry, even in the absence of any mixing with charge-transfer states or asymmetric interactions with the environment, its states could be dipolar. However,  $C_2$  symmetry requires that any electronic asymmetry be along the  $C_2$  axis. Since the  $C_2$  axis is approximately perpendicular to the special pair  $Q_Y$  transition dipole moment direction,<sup>1,57</sup>  $\zeta_A$  would be predicted to be about  $90^\circ$ . Breaking of the intrinsic electronic  $C_2$  symmetry of  $^1P$  by unequal mixing with the charge-transfer states  $P_L^{+}P_M^{-}$  and  $P_M^{+}P_L^{-}$  or unequal mixing with  $P^{+}B_M^{-}$  and  $P^{+}B_L^{-}$  would cause a rotation of the direction of the permanent dipole of  $^1P$ , resulting in a value of  $\zeta_A$  less than  $90^\circ$  and closer to  $31^\circ$  or  $46^\circ$  (assuming that the ground state of P is relatively nonpolar). The extent of such a rotation depends on the magnitude of the intrinsic dipole of the dimer excitonic excited state relative to that provided by mixing with charge-transfer states. The experimental value of  $\zeta_A$  for the special pair  $Q_Y$  transition is  $38 \pm 2^\circ$  (Figure 5B), which demonstrates that the states of the dimer are not those of a perfectly  $C_2$  symmetric molecule. The electronic symmetry of the special pair can, of course, also be affected by interactions with its somewhat asymmetric protein environment. (This is formally equivalent to the statement that certain charge-transfer states are stabilized relative to others.) A satisfactory fit to the  $\zeta_A$  data provides an important target for calculations that seek to understand the nature of the electronic states which are important

(49) Middendorf, T. M.; Gottfried, D. S.; Lockhart, D. J.; Johnson, D. G.; Wasielewski, M. R.; Boxer, S. G. Manuscript in preparation.

(50) Parson, W. W.; Warshel, A. J. *Am. Chem. Soc.* **1987**, *109*, 6152-6163.

(51) Warshel, A.; Creighton, S.; Parson, W. W. *J. Phys. Chem.* **1988**, *92*, 2696-2701.

(52) Sebastian, L.; Weiser, G.; Peter, G.; Bässler, H. *Chem. Phys.* **1983**, *75*, 103.

(53) Sebastian, L.; Weiser, G.; Bässler, H. *Chem. Phys.* **1981**, *61*, 125.

(54) Yoshida, H.; Tokura, Y.; Koda, T. *Chem. Phys.* **1986**, *109*, 375.

(55) Gottfried, D.; Boxer, S. G. Unpublished results.

(56) Scherer, P. O. J.; Fischer, S. F. *Chem. Phys. Lett.* **1986**, *131*, 153-159.

(57) Zinth, W.; Sander, M.; Dobler, J.; Kaiser, W. In *Springer Series in Chemical Physics on Antennas and Reaction Centers of Photosynthetic Bacteria*; Michel-Beyerle, M. E., Ed.; Springer: Berlin, 1985; Vol. 42, p 97.

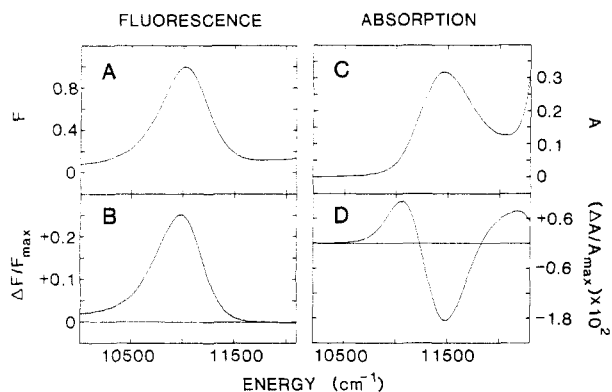


**Figure 7.** (A) Fluorescence spectrum of quinone-depleted *Rb. sphaeroides* RCs in PVA at 77 K in the absence of a field and (B) the change in the fluorescence intensity for the same sample in a field of  $8.9 \times 10^5$  V/cm. (C) Absorption spectrum of the  $Q_y$  transition of the special pair in quinone-depleted reaction centers in PVA at 77 K and (D) the change in the absorbance for the same sample in a field of  $8.9 \times 10^5$  V/cm.

in the initial steps of photosynthesis.

The fact that  $|\Delta\mu_A|$  is not too small and that  $\zeta_A$  equals  $38^\circ$  and not  $90^\circ$  indicates that there is substantially more electron density in the state  $^1P$  along either the L- or M-side (the two sides are not distinguishable from the observable  $\zeta_A$  only); i.e., unidirectional electronic movement begins upon electronic excitation of P. Since the electronic overlap between  $^1P$  and the initial electron acceptor is an important determinant of the rate of electron transfer (through the electronic coupling term  $V$ ), asymmetry in the electronic distribution in  $^1P$  will lead to differences in  $V$  for the two possible electron-transfer pathways, contributing to the observed unidirectionality of the electron-transfer reactions.<sup>20</sup> The absorption Stark effect measurement of  $\zeta_A$  provides direct *experimental* evidence that the electronic distribution in the state  $^1P$  favors electron transfer along one branch over the other.

The quantitative results of the absorption Stark effect measurement favor a model in which the initially excited state of P is quite different from its ground state or the excited state of a monomeric bacteriochlorophyll. The question then is whether the initially populated excited state evolves on a subpicosecond time scale to a state with a still greater degree of charge separation, as suggested by one interpretation of the hole-burning data. In order to investigate this question, we measured the Stark effect on the weak fluorescence from the special pair.<sup>58</sup>  $|\Delta\mu_F|$  would be much larger than  $|\Delta\mu_A|$  if  $^1P$  decays on a subpicosecond time scale into a pure charge-transfer state<sup>26</sup> because in this case most of the fluorescence (which has a several picosecond lifetime as measured by the time dependence of the stimulated emission<sup>9-11</sup>) would come from this more dipolar state.<sup>119</sup> Conversely,  $|\Delta\mu_F|$  should be comparable to  $|\Delta\mu_A|$  if the  $^1P$  state does not evolve on a subpicosecond time scale. The results for *Rb. sphaeroides* are shown in Figure 7;<sup>58</sup> similar results have been obtained for *Rps. viridis* and *Rb. capsulatus* RCs.<sup>120</sup> Rather than the expected second-derivative line shape for a Stark effect due to  $\Delta\mu_F$ , we observe a primarily zeroth-derivative line shape, i.e., the *overall fluorescence yield increases in the applied field*. This new effect dominates the expected second-derivative-shaped Stark effect, thwarting attempts to measure  $|\Delta\mu_F|$  directly. However, a model calculation that takes this new effect on the fluorescence yield into account indicates that if  $|\Delta\mu_F|$  were larger than about 10 D, the line shape of the  $\Delta F$  spectrum would be significantly different than observed.<sup>58,59</sup> This argues against evolution of the initial dimer excited state into a more dipolar, charge-transfer state on a subpicosecond time scale.

**Effects of an Electric Field on the Rates of Electron-Transfer Reactions.** The observed zeroth-derivative shape of the change in fluorescence shown in Figure 7B suggests that an entirely

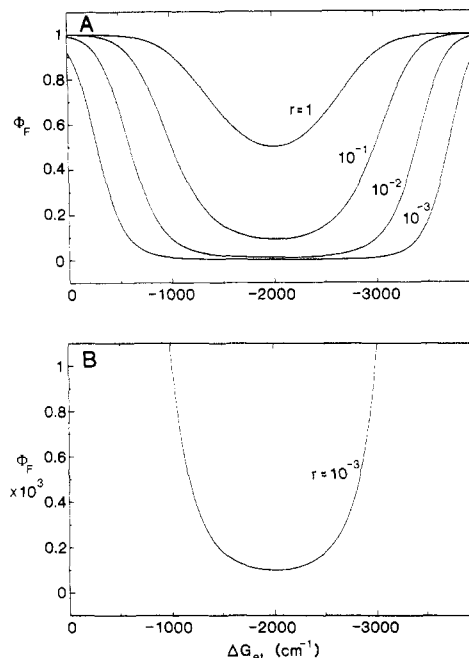


**Figure 8.** Dependence of the fluorescence quantum yield,  $\Phi_F = k_F/(k_F + k_{et})$ , on  $\Delta G_{et}^0$  using the semiclassical Marcus expression<sup>61</sup> for  $k_{et}$  with  $\lambda = 2000$  cm<sup>-1</sup>. Plots are shown for different values of  $k_F$  relative to the maximum value of  $k_{et}$ , i.e.,  $r = k_F/k_{et}(\max)$ . The lower panel is an expansion of the upper plot for  $r = 10^{-3}$ , a situation believed to be relevant to RCs.

different mechanism is dominant than for the conventional Stark effect, and this has led to the development of a new method for probing electron-transfer reactions. Consideration of the reaction scheme in Figure 4 suggests that the fluorescence would increase if processes competing with fluorescence slow down. The rate of the forward electron-transfer reaction is expected to depend on electric field strength because of the electric field dependence of the energy of the dipolar product state,  $P^{*+}I^{-}$ , as illustrated in Figure 4, where  $P^{*+}I^{-}$  is the state whose formation competes with the fluorescence from  $^1P$ , and  $I$  is either B or H. For example, the energy of a state with a 50-D dipole moment (charge separated by 10 Å) will change by about 100 meV (800 cm<sup>-1</sup>) if the dipole is aligned with a field of  $1 \times 10^6$  V/cm. This is a substantial change relative to the zero-field driving force,  $\Delta G_{et}^0$ , of the electron-transfer reaction  $^1PH \rightarrow P^{*+}H^{-}$  (see below).

There have been many theoretical treatments analyzing the effect of driving force on electron-transfer rates, beginning with the pioneering work of Marcus.<sup>60,61</sup> Nonadiabatic electron-transfer theories generally give an expression for  $k_{et}$  with the form

$$k_{et} = (4\pi^2/h)|V|^2 FC \quad (2)$$

where  $V$  is the electronic interaction matrix element and FC is the thermally averaged Franck-Condon weighted density of states.  $V$  depends on the overlap of the wave functions of the donor and acceptor and is the dominant source of the distance dependence of electron transfer. FC can be treated either in a semiclassical manner or in a variety of more sophisticated ways and gives rise to the dependence of  $k_{et}$  on the driving force for electron transfer,  $\Delta G_{et}^0$ , and on the reorganization energy. During the past several years, the applicability of Marcus theory and its descendants to electron transfer in the RC has been widely discussed.<sup>8,12,20,61,62</sup>

In order to explain qualitatively the net increase in fluorescence in an electric field, there must be a net decrease in  $k_{et}$ , the rate of the competing initial charge-separation reaction. In principle, the applied field could affect both  $V$  and FC; we consider the simpler effect on FC first. In an isotropic RC sample the applied field produces a range of values of  $\Delta G_{et}^0$  symmetrically disposed

(58) Lockhart, D. J.; Boxer, S. G. *Chem. Phys. Lett.* **1988**, *144*, 243.

(59) Lockhart, D. J.; Boxer, S. G. *J. Phys. Chem.*, submitted for publication.

(60) Marcus, R. A. *J. Chem. Phys.* **1956**, *24*, 966-978.

(61) Marcus, R. A.; Sutin, N. *Biochim. Biophys. Acta* **1985**, *811*, 265-322.

(62) Jortner, J. *J. Am. Chem. Soc.* **1980**, *102*, 6676-6686.



around the zero-field value. This range of  $\Delta G^\circ_{\text{et}}$  values maps in some nonlinear way onto a range of values of  $k_{\text{et}}$  depending on the exact form of FC. We observe the fluorescence quantum yield,  $\Phi_F = k_F/(k_F + k_{\text{et}})$ , where  $k_F$  is the radiative rate of  $^1\text{P}$  which is assumed to be independent of field.<sup>121</sup> The calculated dependence of  $\Phi_F$  on  $\Delta G^\circ_{\text{et}}$  is plotted in Figure 8, using a semiclassical Marcus theory expression for FC. It is seen that the applied field will always produce an increase in  $\Phi_F$  for an isotropic sample so long as the zero-field magnitude of  $\Delta G^\circ_{\text{et}}$  is not too different from the reorganization energy. This is because the curvature of the  $\Phi_F$  vs  $\Delta G^\circ_{\text{et}}$  curve in this region is such that the increase in  $\Phi_F$  for RCs oriented in a given direction relative to the field is always greater than the decrease in  $\Phi_F$  for RCs oriented oppositely. The amount by which the zero-field value of  $\Delta G^\circ_{\text{et}}$  can differ from the reorganization energy for there to be an increase of  $\Phi_F$  in a field depends on the relative values of  $k_F$  and  $k_{\text{et}}$ . If  $k_F \ll k_{\text{et}}$  at zero field, as is the case in the RC, then an increase in  $\Phi_F$  is expected for an isotropic sample in an electric field unless the zero-field values of  $\Delta G^\circ_{\text{et}}$  and the reorganization energy differ in magnitude by more than 1000 cm<sup>-1</sup>. More realistic treatments of FC will change the shape and symmetry of these curves about  $-\Delta G^\circ_{\text{et}} = \lambda$ , but the prediction regarding the sign of the change in fluorescence in an applied field for an isotropic sample will hold.

It would be very desirable to have information on the exact form of the  $k_{\text{et}}$  vs  $\Delta G^\circ_{\text{et}}$  curve for the initial electron-transfer reaction in the RC in order to be able to calculate the expected magnitude of  $\Delta F_{\text{et}}/F$ . This information could be obtained by studying the effect of a field on electron-transfer kinetics in an isotropic<sup>63,64</sup> or an oriented<sup>65-67</sup> sample. Dutton and co-workers have approached this problem using RCs oriented in Langmuir-Blodgett films.<sup>65-67</sup> These investigators observed a decrease in the apparent quantum yield of  $\text{P}^{++}\text{Q}_\text{A}^-$  formation in an applied electric field. Unfortunately, there is no simple way to compare this interesting result with our fluorescence data because the  $\text{P}^{++}\text{Q}^-$  quantum yield reflects several competing electron-transfer steps:  $^1\text{PHQ}_\text{A} \rightarrow \text{P}^{++}\text{H}^-\text{Q}_\text{A}$ ;  $\text{P}^{++}\text{H}^-\text{Q}_\text{A} \rightarrow \text{P}^{++}\text{HQ}_\text{A}^-$ ;  $\text{P}^{++}\text{H}^- \rightarrow \text{P}$ ; and  $\text{P}^{++}\text{H}^- \rightarrow ^3\text{P}$  (see Figures 1 and 3), each of which may be sensitive to the field. The fluorescence electric field effect experiment is sensitive only to reactions that directly compete with the emission. However, a potentially serious problem with interpreting the absolute magnitude of  $\Delta F_{\text{et}}/F$  is that there may be contamination of the weak fluorescence with fluorescence from RCs whose special pair is intact but whose function is somehow degraded, in which case the observed value of  $\Delta F_{\text{et}}/F$  would be a lower limit to the true value. (The local field correction introduces further uncertainty.<sup>117</sup>) In order to address this problem, we have recently initiated studies of the effect of an applied field on the kinetics of the initial electron-transfer reaction in an isotropic sample in collaboration with Kirmaier and Holten.<sup>68,69</sup> The results demonstrate a small effect on the picosecond charge separation kinetics (the net decay is slower in the field); the change in the decay kinetics is consistent (within a factor of 2) with the magnitude of the change in fluorescence. Thus, it appears that the magnitude of  $\Delta F_{\text{et}}/F$  is a reliable indicator of the field effect on  $k_{\text{et}}$ . Furthermore, this result indicates that the reduction in  $\text{P}^{++}\text{Q}_\text{A}^-$  quantum yield observed in Dutton's experiments described above<sup>67</sup>

is not likely due to a reduction in the rate of the  $^1\text{PHQ}_\text{A} \rightarrow \text{P}^{++}\text{H}^-\text{Q}_\text{A}$  initial step.

For a given RC, the relative energies of the states  $\text{P}^{++}\text{B}_\text{L}^-$ ,  $\text{P}^{++}\text{B}_\text{M}^-$ ,  $\text{P}^{++}\text{H}_\text{L}^-$ , and  $\text{P}^{++}\text{H}_\text{M}^-$  will change in an electric field, the magnitude and direction of the changes depending on the orientation of the RC in the field. For example, by chance it turns out that the dipoles of the states  $\text{P}^{++}\text{B}_\text{L}^-$  and  $\text{P}^{++}\text{B}_\text{M}^-$  are nearly antiparallel. As a result, in a field of 10<sup>6</sup> V/cm the energy of the state  $\text{P}^{++}\text{B}_\text{L}^-$  can be increased by as much as about 860 cm<sup>-1</sup> while in the same RC the energy of the state  $\text{P}^{++}\text{B}_\text{M}^-$  will be decreased by about 780 cm<sup>-1</sup>. Despite these relatively large energetic changes, to within the limits of sensitivity ( $\sim 10\%$ ) there was no evidence for electron transfer down the M-branch for an isotropic sample in a field of 10<sup>6</sup> V/cm.<sup>68,69</sup> Apparently, unidirectional electron transfer is not the result of small differences in the energies of the charge-separated M- and L-side states.

**The Identity of the Initial Electron Acceptor: Orientation Dependence of Electric Field Effects.** Since  $\Delta G^\circ_{\text{et}}$  and hence  $k_{\text{et}}$  depend on the angle between the internal dipoles in the RC and the externally applied electric field through the term  $\Delta\mu_{\text{et}}\cdot\mathbf{F}_{\text{int}}$ , one predicts that the change in  $k_{\text{et}}$  with field must depend on the orientation of the RC in the field. For a randomly oriented sample excited isotropically at zero applied field, the fluorescence is isotropic. However, if the rate of the initial electron-transfer reaction that competes with the fluorescence depends on the orientation of the RCs in the field, then the fluorescence should become polarized as the field is applied (electric-field-induced fluorescence anisotropy). Neglecting for the moment possible field effects on  $V$ , it can be shown that the angle dependence of  $\Delta F_{\text{et}}$  has a form analogous to eq 1:<sup>28</sup>

$$\Delta F_{\text{et}}(\chi) \propto 5 + (3 \cos^2 \chi - 1)(3 \cos^2 \zeta_{\text{et}} - 1) \quad (3)$$

where  $\zeta_{\text{et}}$  is the angle between the transition dipole of the fluorescence transition and the dipole moment of the electron-transfer product state,  $\Delta\mu_{\text{et}} = \mu(\text{P}^{++}\text{I}^-) - \mu(^1\text{PI}) \sim \mu(\text{P}^{++}\text{I}^-)$  (Figure 4), and  $\chi$  is the experimental angle between the applied electric field and the polarization direction of an analyzing polarizer through which the fluorescence is collected. Equation 3 can be derived if the dependence of  $k_{\text{et}}$  on  $\Delta G^\circ_{\text{et}}$  is given by the semiclassical Marcus expression. In addition, eq 3 also results if one uses any relationship between  $k_{\text{et}}$  and  $\Delta G^\circ_{\text{et}}$  that can be fit to a general third-order polynomial in the field-induced perturbation,  $\Delta\mu_{\text{et}}\cdot\mathbf{F}_{\text{int}}$ , over the range of the curve sampled in the presence of the field (this can be made very small commensurate with suitable signal-to-noise), making the analysis independent of any particular electron-transfer model. (It is not necessary that the actual fitting function be known, but only that such a fit is possible.) Equation 3 suggests an approach to measuring the direction of the dipole moment of the ion-pair state which is generated in an electron-transfer reaction (i.e., the direction of electron movement) by measuring the variation of  $\Delta F_{\text{et}}$  as a function of the experimental angle  $\chi$ . The experimentally determined value of  $\zeta_{\text{et}}$  is then combined with geometric information from the RC crystal structure to obtain information on the identity of the initial electron acceptor.

The results of measurements of the angle dependence of the electric field effect on the fluorescence are shown in Figure 5A. It is seen that whereas  $\zeta_F \sim \zeta_A$  for bacteriochlorophyll *a* as expected for an aromatic molecule in which there are no significant electric-field-dependent pathways which compete with fluorescence,  $\zeta_{\text{et}}$  is much greater than  $\zeta_A$  for the special pair in *Rb. sphaeroides* RCs.  $\zeta_F$  for BChl *a* and  $\zeta_{\text{et}}$  for the RC measure different internal angles because the mechanism of the electric field effect on the emission is very different in the two cases.  $\zeta_{\text{et}}$  for the RC is measured to be  $69 \pm 4^\circ$ .

The direction of the transition dipole moment can be obtained from single-crystal polarized absorption spectroscopy<sup>57</sup> or theoretical calculations,<sup>50,70</sup> and it has been shown that the fluorescence

(63) Boxer, S. G.; Goldstein, R. A.; Franzen, S. In *Photoinduced Electron Transfer*; Fox, M. A., Chanan, M., Eds.; Elsevier Press: Amsterdam, 1988; Vol. B, pp 163-215.

(64) Boxer, S. G.; Lockhart, D. J.; Franzen, S. In *Photochemical Energy Conversion*; Norris, J. R., Jr., Meisel, D., Eds.; Elsevier Press: Amsterdam, 1989; pp 196-210.

(65) Dutton, P. L.; Alegria, G.; Gunner, In *The Photosynthetic Bacterial Reaction Center—Structure and Dynamics*; Breton, J., Vermeglio, A., Eds.; Plenum: New York, 1988; pp 185-194.

(66) Popovic, Z. D.; Kovacs, G. J.; Vincett, P. S.; Alegria, G.; Dutton, P. L. *Biochim. Biophys. Acta* **1986**, *851*, 38.

(67) Popovic, Z. D.; Kovacs, G. J.; Vincett, P. S.; Alegria, G.; Dutton, P. L. *Chem. Phys.* **1986**, *110*, 227.

(68) Boxer, S. G.; Lockhart, D. J.; Kirmaier, C.; Holten, D. In *Perspectives in Photosynthesis*; Jortner, J., Pullman, B., Eds.; Elsevier: Amsterdam, in press.

(69) Lockhart, D. J.; Kirmaier, C.; Hoten, D.; Boxer, S. G. *J. Phys. Chem.*, submitted for publication.

(70) Plato, M.; Lendzian, F.; Lubitz, W.; Trankle, E.; Mobius, K. In *The Photosynthetic Bacterial Reaction Center—Structure and Dynamics*; Breton, J., Vermeglio, A., Eds.; Plenum: New York, 1988; pp 379-388.



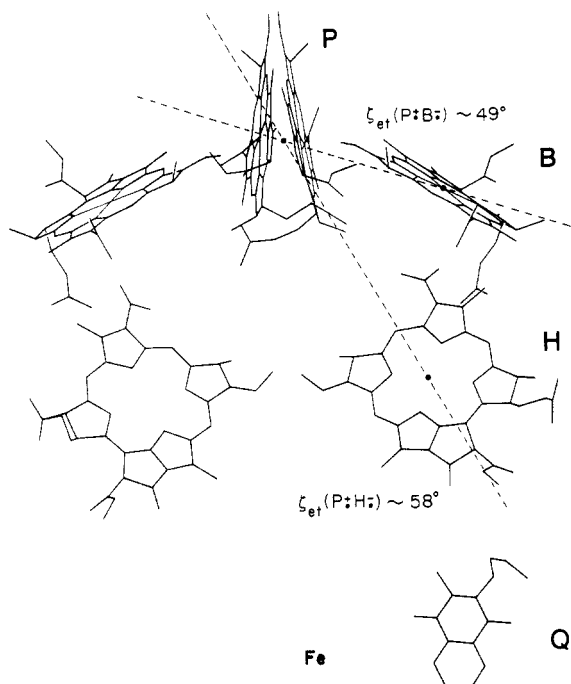


**Figure 9.** Arrangement of the chromophores participating in the initial electron-transfer reaction taken from the X-ray coordinates for *Rps. viridis* reaction centers (ref 1–3). A nearly identical figure is obtained for *Rb. sphaeroides* (see ref 4–6). The absorption (fluorescence) transition moment direction is approximately perpendicular to the page passing through the point at the geometric center of the special pair (P). The angle  $\zeta_{et}$  is between the direction of the transition moment and a line drawn from the geometric center of P to that of either B or H using the coordinates from the crystal structure of *Rps. viridis* (see Table I and ref 122). This figure is for the purpose of illustration only. No two-dimensional representation can adequately represent this three-dimensional problem.

and absorption transition moments are nearly parallel.<sup>71</sup> The direction of the  $P^{+}B^{-}$  or  $P^{+}H^{-}$  dipole moment can be estimated from the X-ray structure, assuming that the charge in the ions can be approximated by point charges at the geometric centers of the chromophores.<sup>122</sup> The results of such estimates are shown in Figure 9. If  $P^{+}B^{-}$  formation competes with fluorescence,  $\zeta_{et}$  is predicted to be about 49°, significantly different than what is observed. This result argues that formation of  $P^{+}B^{-}$  does not compete with fluorescence from  $^1P$ , so  $P^{+}B^{-}$  cannot be a discrete intermediate in electron transfer. A similar conclusion has been reached from the interpretation of subpicosecond transient absorption experiments.<sup>13,14</sup> Although the measured value of  $\zeta_{et}$  is considerably closer to what is predicted for direct formation of  $P^{+}H^{-}$ , the observed angle is even larger. (The predicted values of  $\zeta_{et}$  in Figure 9 ignore the possibility that  $^1P$  is somewhat dipolar.<sup>122</sup>)

**Effect of an Electric Field on the Electronic Coupling—Superexchange.** Until now we have assumed that the electric field only affects FC (eq 2) through the change in  $\Delta G_{et}$  and that the electronic coupling matrix element  $V$  is independent of electric field. In this case,  $V$  depends on the interaction of the orbitals on the donor ( $^1P$ ) and acceptor (H). Its absolute value is difficult to calculate because the tails of the wave functions on the donor and acceptor are not known accurately, though several treatments have been published.<sup>20,51,56,72,73</sup> The electronic interaction between the donor and acceptor could change in an applied field, the magnitude of the change depending on the difference in the polarizability between the donor and the acceptor states. This is likely to lead to only a small effect relative to the effect due to

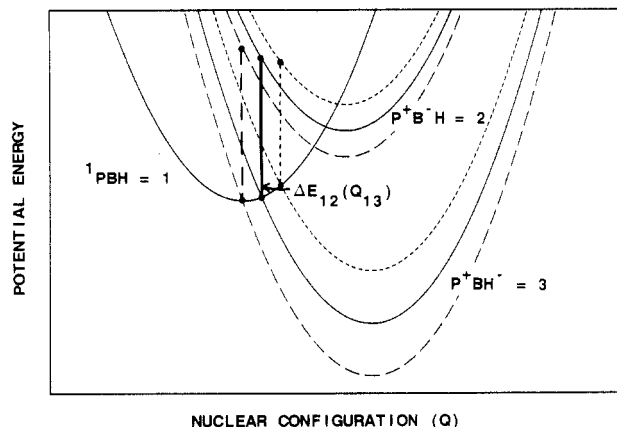


**Figure 10.** Schematic illustration of the relevant potential energy curves as a function of nuclear configuration for a superexchange mechanism for the initial electron-transfer reaction in the RC. State 1 =  $^1PBH$ ; state 2 = mediating state, e.g.,  $P^{+}B^{-}H$  or  $P^1BH$ ; state 3 =  $P^{+}BH^{-}$ . (—) Zero-field curves for the initial, mediating, and final states. Potential energy curves in the presence of an electric field which is aligned (---) or opposed (- - -) to the permanent dipole moment of the final state. It is assumed that the dipole moment of the initial state is negligible and that the dipole moment of the mediating state is half as large as that of the final state and in the same direction.  $Q_{13}$  is the value of  $Q$  at which the curves for the initial and final states cross along the relevant reaction coordinate, and  $\Delta E_{12}(Q_{13})$  is the vertical energy difference between curves 1 and 2 at this value of  $Q_{13}$ . Note that moving the curve for state 3 vertically relative to that for state 1 (a change in  $\Delta G_{et}$ ) changes  $Q_{13}$  and thus  $\Delta E_{12}(Q_{13})$ , even if the curve for state 2 remains fixed (as would be the case if state 2 is relatively nonpolar, e.g., if state 2 is  $P^1BH$ ). The qualitative features of the figure are expected to be generally applicable to long-distance electron-transfer reaction between neutral molecules. For long-distance electron-transfer reactions between two sites separated by molecules in the intervening medium (e.g., aromatic or aliphatic spacers, solvent molecules, amino acids), the possibility exists for participation by states involving the medium. In these cases, the mediating state is likely to be intermediate in overall nuclear configuration between the initial and final state and the dipole of the mediating state (if it is dipolar) is likely to be intermediate in magnitude and approximately parallel to that of the final state.

the change in the energies of very dipolar states discussed in the previous section, though definitive experiments need to be developed to prove this point.

A more interesting situation arises if the electronic coupling between donor and acceptor is mediated by states of the intervening medium, e.g., by superexchange. For convenience, we introduce the following notation (see Figure 10): state 1 =  $^1PBH$ ; state 2 = mediating state, e.g.,  $P^{+}B^{-}H$  or  $P^1BH$ ; state 3 =  $P^{+}BH^{-}$ . In such a model the electronic coupling between the initial and final states of the electron-transfer reaction is enhanced by virtue of electronic coupling between the initial and mediating state,  $V_{12}$ , and between the mediating and final state,  $V_{23}$ . The overall electronic coupling,  $V_{et}$ , also depends on the energy difference,  $\Delta E_{12}$ , between the initial state and the mediating state at the nuclear configuration of the crossing of the potential energy surfaces of the initial and final state,  $Q_{13}$  (see Figure 10). Treating the problem by perturbation theory<sup>20,72–74</sup>

$$V_{et} = \frac{V_{12}V_{23}}{\Delta E_{12}(Q_{13})} \quad (4)$$

where

$$V_{12} = \langle 1 | \mathcal{H}_1 | 2 \rangle$$

$$V_{23} = \langle 2 | \mathcal{H}_1 | 3 \rangle$$

$$\Delta E_{12}(Q_{13}) = E_2(Q_{13}) - E_1(Q_{13}) \gg V_{12}$$

$\mathcal{H}_1$  is the Hamiltonian of the interaction which couples the states, and  $\Delta E_{12}(Q_{13})$  is the energy difference between the initial state

(71) Ebrey, T. G.; Clayton, R. K. *Photochem. Photobiol.* **1969**, *10*, 109.

(72) Plato, M.; Möbius, K.; Michel-Beyerle, M. E.; Bixon, M.; Jortner, J. *J. Am. Chem. Soc.* **1988**, *110*, 7279–7285.

(73) Bixon, M.; Jortner, J.; Michel-Beyerle, M.; Ogrodnik, A.; Lersch, W. *Chem. Phys. Lett.* **1987**, *140*, 622–630.

(74) Bixon, M.; Jortner, J. *J. Phys. Chem.* **1988**, *92*, 7148–7156.

and the mediating state at the nuclear configuration of the intersection of the electron-transfer initial- and final-state potential surfaces,  $Q_{13}$  (not the energy difference between the states at their individual equilibrium nuclear configurations).

In addition to the field effect on FC (through a change in the energy of  $P^{*+}H^{-}$  leading to a change in  $\Delta G_{et}$ ), an electric field can also affect  $V_{et}$  by changing  $\Delta E_{12}$  in two ways: (1) the energy of the mediating state is changed by the field (this is especially important if the mediating state is very dipolar); (2) a change in  $\Delta G_{et}$  also results in a change in  $Q_{13}$ .<sup>75</sup> Since the initial- and mediating-state potential energy surfaces are not flat,  $\Delta E_{12}(Q_{13})$  changes because the value of  $Q_{13}$  changes. As a result,  $\Delta E_{12}$  can be field dependent due to a dipolar final state, even if the mediating state is nonpolar. Specifically, assuming that the potential energy curves for the initial, mediating, and final states are harmonic and that they have the same shape, in an electric field  $F_{int}$  (see Figure 10)

$$\Delta E_{12}(F_{int}) = \Delta E_{12}(F_{int}=0) - \mu(2) \cdot F_{int} + (\lambda_{12}/\lambda_{13})^{1/2} [\mu(3) \cdot F_{int}] \quad (5)$$

where  $\lambda_{ij}$  is the reorganization energy (a measure of the difference in equilibrium nuclear configuration) between states  $i$  and  $j$ .<sup>69</sup>

The superexchange mechanism has been considered in detail by a number of investigators, always in the context of the role played by  $P^{*+}B^{-}$  in mediating the coupling between  $^1P$  and  $P^{*+}H^{-}$ .<sup>20,72-74,76,77</sup> Bixon and Jortner have recently considered the effects of electric fields in this model, for both isotropic and oriented systems.<sup>74</sup> Assuming that  $P^{*+}B^{-}$  is the key mediating state, the calculated value of  $\Delta F_{et}/F$  for reasonable values of the parameters involved is considerably larger (by about an order of magnitude) than what we have observed for a field of  $10^6$  V/cm. Furthermore, the calculated dependence of  $\Delta F_{et}/F$  on field<sup>74</sup> is very different from what is observed.<sup>28</sup> The only effect of the field on  $V_{et}$  that is modeled in ref 74 is that mentioned in (1) in the previous paragraph, namely

$$V_{et} = V_{12}V_{23}/[\Delta E_{12}(Q_{13}) - \mu(P^{*+}B^{-}) \cdot F_{int}] \quad (6)$$

where  $\Delta E_{12}(Q_{13})$  is the zero-field value (i.e., independent of field). However, if one uses the same zero-field parameters, the effects outlined in (2) lead to a significant *reduction* in the calculated effect of the field on the fluorescence yield,<sup>69</sup> i.e., the additional effect of the field on  $V_{et}$  tends to mitigate the effect of the field on FC. The extent to which the effects in (2) mitigate or enhance the effects of the field on FC depends on the specific properties of the states (namely, the zero-field  $\Delta G$  values and reorganization energies, the magnitude and directions of permanent dipole moments, and the nuclear potential energy surfaces). At the present time there is no direct information on the shapes of the potential energy surfaces or the energy of states such as  $P^{*+}B_L^{-}$ . Note that the qualitative features discussed here and illustrated in Figure 10 are expected to be generally applicable to any long-distance electron transfer between neutral molecules. For long-distance electron-transfer reactions between two sites separated by molecules in the intervening medium (e.g., aromatic or aliphatic spacers, solvent molecules, amino acids), the possibility exists for participation by states involving the medium. In these cases, the mediating state is likely to be intermediate in overall nuclear configuration between the initial and final state, and the dipole of the mediating state (if it is dipolar) is likely to be intermediate in magnitude and approximately parallel to that of the final state.

An alternative possibility is that the state which mediates the interaction between  $^1P$  and  $P^{*+}H^{-}$  is not  $P^{*+}B^{-}$  but rather a neutral excited state such as  $^1B$ . ( $^1B$  is the lowest energy singlet electronic excited state of  $B$ .) Whereas there is no direct information on the energy of the state  $P^{*+}B^{-}$  (a major difficulty in any quantitative assessment of a mechanism involving  $P^{*+}B^{-}$ ), we know from the absorption spectrum that the state  $^1B$  in *Rb*.

*sphaeroides* is not far in energy ( $\sim 1100$  cm<sup>-1</sup>) above  $^1P$ . In this case, effect (1) is unimportant because the mediating state is approximately nonpolar, but effect (2) can still cause  $\Delta E_{12}$ , and thus  $V_{et}$ , to be field dependent. A quantitative assessment of these cases is presented elsewhere.<sup>69</sup> If the mediating state is  $^1B$ , the effects due to mechanisms (1) and (2) are not expected to counteract each other, and one has the somewhat counterintuitive possibility that larger electric field effects may result with a neutral rather than dipolar mediating state. The magnitude of the overall electronic coupling,  $V_{et}$  (eq 4), may be smaller if  $^1B$  is the mediating state than if  $P^{*+}B^{-}$  is the mediating state. ( $V_{23}$  is likely to be smaller, but  $V_{12}$  may be larger.)

As discussed above, the magnitude (but not the angle dependence) of the effect of an electric field on the fluorescence could be compromised by fluorescence from impaired RCs; however, the recent measurement of the effect of the field on the kinetics of the initial step in an isotropic sample confirms that the observed magnitude of  $\Delta F_{et}/F$  primarily reflects the change in  $k_{et}$ .<sup>68,69</sup> The only remaining uncertainty is the local field correction;<sup>117</sup> however, this factor would have to be very different from what is ordinarily expected in order to resolve the discrepancy between the electric field effect calculated by Bixon and Jortner<sup>74</sup> and the experimental results.<sup>28,58,68,69</sup> Thus, the experimentally determined magnitude of  $\Delta F_{et}/F$  at least places limits on the values of the parameters used in the superexchange model. Other general objections to the superexchange mechanism have been presented by Marcus,<sup>78,79</sup> Won and Friesner<sup>76</sup> have shown that interesting effects can arise if a charge-transfer state of  $P$  (e.g.,  $P^{*+}P^{-}$ ) is nearly resonant with the lower exciton state of  $P$ .

As stated above, the magnitude of the electric field effect on the fluorescence,  $\Delta F_{et}/F$ , calculated by Bixon and Jortner<sup>74</sup> using a superexchange model and a field of  $10^6$  V/cm is larger by more than an order of magnitude than the observed value.<sup>28</sup> The inclusion of the effect on  $V_{et}$  due to a field-dependent value of  $Q_{13}$  (see Figure 10) can reduce the calculated value of  $\Delta F_{et}/F$  by about 30% for a field of  $10^6$  V/cm, using the zero-field parameters in ref 74, but the calculated value is still much larger than that observed experimentally.<sup>28,58,69</sup> Although the field dependence of  $V$  can be significant, the effect of the field on FC (through  $\Delta G_{et}$ ) is expected to be dominant if one uses the dependence of FC on  $\Delta G_{et}$  given by the commonly used versions of conventional electron-transfer theories<sup>61</sup> and assuming that  $\Delta G_{et}$  changes as  $-\mu(P^{*+}H^{-}) \cdot F_{int}$ . In other words, FC is expected to be strongly dependent on field because the state  $P^{*+}H^{-}$  is very dipolar ( $\mu(P^{*+}H^{-}) \sim 80$  D), and the simplified treatments commonly in use predict a large change in FC for such a large change in  $\Delta G_{et}$ . Therefore, if the dependence of FC on  $\Delta G_{et}$  used to predict electric field effects in the RC is too steep, the predicted values of  $\Delta F_{et}/F$  will tend to be too large regardless of the specific mechanism being modeled or the specific treatment of the field dependence of  $V$ . It appears that a more sophisticated treatment of the dependence of FC on  $\Delta G_{et}$  that takes into account the specific components in the RC is now warranted by the apparent inability of the simple treatments to predict the experimentally observed electric field effects.<sup>59,69</sup>

**Absorption Stark Effect Line Shape Revisited.** As discussed earlier, the absence of a first-derivative contribution to the special pair  $Q_Y$  band absorption Stark signal places additional constraints on the energies and coupling strengths of charge-transfer states. In the following we discuss several possibilities and describe the conditions under which they are consistent with these constraints. Let  $^1P_{ex}$  be the pure excitonic excited state of  $P$  in the absence of any mixing with other states; the state  $^1P$  is a linear combination of  $^1P_{ex}$  and any states to which it is coupled (specifically, charge-transfer states). If the relevant charge-transfer states are higher in energy than  $^1P_{ex}$ , then the absence of a first-derivative contribution means that the coupling to these charge-transfer states must be very weak (in order to be unimportant) or very strong (in order to be essentially unchanged by the field). Alternatively,

(75) Mikkelsen, K. V.; Ulstrup, J.; Zakaraya, M. G. *J. Am. Chem. Soc.* **1989**, *111*, 1315-1319.

(76) Won, Y.; Friesner, R. A. *Biochim. Biophys. Acta* **1988**, *935*, 9-18.

(77) Bixon, M.; Michel-Beyerle, M. E.; Jortner, J. *Isr. J. Chem.* **1988**, *28*, 155-168.

(78) Marcus, R. A. *Chem. Phys. Lett.* **1987**, *133*, 471-477.

(79) Marcus, R. A. *Chem. Phys. Lett.* **1988**, *146*, 13-21.

the energy separation between the excitonic state of P and the relevant charge-transfer states must be large relative to the electric field perturbation,  $-\Delta\mu_{CT}F$  (where  $\Delta\mu_{CT}$  is the dipole moment difference between the relevant charge-transfer state and  $^1P_{ex}$ ). The last alternative is unlikely based on estimates of the energies of states such as  $P^{+}P^{-}$  or  $P^{+}B^{-}$  by Warshel and Parson<sup>50</sup> and what is known about the redox properties of the chromophores. The very weak coupling possibility is unlikely based on the observation that  $|\Delta\mu_A|$  for the special pair (as determined by the absorption Stark effect measurements) is considerably larger than for monomeric bacteriochlorophyll,<sup>45</sup> which suggests that mixing with charge-transfer states is not negligible.

We now consider the case of strong coupling to higher energy charge-transfer states in greater detail. If the relevant CT states are  $P^{+}B_L^{-}$  and  $P^{+}B_M^{-}$ , then with strong coupling the  $^1P$  state would be expected to be very dipolar ( $|\mu(P^{+}B^{-})| \sim 50$  D). If  $P^{+}B_L^{-}$  and  $P^{+}B_M^{-}$  contributed equally to  $^1P$ , then  $\mu(^1P)$  would be along the  $C_2$  axis (see Figure 1). If  $P^{+}B_L^{-}$  and  $P^{+}B_M^{-}$  contributed unequally, then  $\mu(^1P)$  would be rotated away from the  $C_2$  axis toward either the L or M side. Large but unequal contributions from the states  $P^{+}B_L^{-}$  and  $P^{+}B_M^{-}$  are unlikely based on the results of absorption Stark effect measurements on  $NaBH_4$ -treated RCs in which  $B_M$  has been either removed or greatly modified.<sup>80</sup> The results indicate that the properties of  $^1P$  are largely unchanged in these modified RCs.<sup>81</sup> Since  $\mu(^1P)$  has been determined (assuming that the ground state of P is relatively nonpolar<sup>18</sup>) to be small relative to 50 D, a large contribution from states such as  $P^{+}B^{-}$  to the properties of the initial excited state of P seems to be unlikely. Next consider strong coupling to the intradimer charge-transfer states  $P_M^{+}P_L^{-}$  and  $P_L^{+}P_M^{-}$ . If these states make equal contributions to  $^1P$  and their dipoles can be described by vectors connecting the centers of the macrocycles, then  $^1P$  would *not* be dipolar due to this mixing because the dipole due to one exactly cancels the other. (Note that this is not true for the states  $P^{+}B_L^{-}$  and  $P^{+}B_M^{-}$  since these two dipoles are not antiparallel, but instead have nonzero projections in the same direction along the  $C_2$  axis.) Thus, the observed permanent dipole of the state  $^1P$  could be due to large but unequal mixing with the intradimer charge-transfer states. This is consistent with the strong mixing picture required for an absence of electric-field-induced changes in mixing as well as the relatively small value of  $\mu(^1P)$ . For the states  $P_M^{+}P_L^{-}$  to make unequal contributions to  $^1P$ , the  $C_2$  symmetry of the system must be broken by the protein environment. This argument suggests that the protein determines the electronic nature of the special pair excited state by determining the energies of the coupled states, a theme which has been developed in some theoretical treatments.<sup>20,50</sup>

An alternative explanation that does not require very strong coupling between  $^1P_{ex}$  and the charge-transfer states is possible in the case that the relevant charge-transfer states are nearly degenerate with  $^1P_{ex}$  or if  $^1P_{ex}$  is intermediate in energy between states with dipoles in opposite directions. These rather special circumstances may arise in the RC because of its unique structural and energetic features. If only a single charge-transfer state is degenerate with  $^1P_{ex}$  and all others can be neglected, then field-induced changes in mixing would lead to a line-broadening (second derivative) contribution in addition to that expected due to a permanent dipole moment difference and not a line shift (first derivative) contribution. If two charge-transfer states with dipoles in opposite directions (for example,  $P_L^{+}P_M^{-}$  and  $P_M^{+}P_L^{-}$ ) are both nearly degenerate with  $^1P_{ex}$  or if  $^1P_{ex}$  is intermediate in energy between such states, then field-induced mixing effects can at least partially cancel leading to little, if any, additional first- or second-derivative contributions to the absorption Stark effect spectrum (but possibly leading to small contributions that are not simply described by a derivative of the absorption band). In addition, in both of the above cases, the nature of the state  $^1P$  is

field dependent because of the field-induced changes in the contributions to the state  $^1P$  from the charge-transfer states. As a result, a zeroth-derivative contribution to the absorption Stark effect spectrum is possible because of a field-induced change in the oscillator strength for the transition between the ground state and  $^1P$ . An analysis of the absorption Stark effect line shape shows that, although close, it is not perfectly described by the second derivative of the absorption spectrum (as would be expected if the only effect were that due to  $\Delta\mu_A$ ).<sup>47,81</sup> This small deviation could be due to the presence of small additional contributions from the mechanisms outlined above. A more radical proposal is that the absorption band giving rise to the strong absorption Stark effect in the vicinity of the P band is actually associated with a much weaker underlying transition with a very large  $|\Delta\mu_A|$ , e.g., a pure charge-transfer state such as  $P^{+}P^{-}$ . Recent measurements of the Stark effect for *Rb. capsulatus*<sup>82</sup> and *Rb. sphaeroides*<sup>83</sup> RCs which contain a heterodimer in the place of P may shed light on this question. (The heterodimer consists of one BChl *a* and one BPheo *a* molecule and is formed by replacing the histidine ligand to the M-side BChl of the special pair with leucine by site-specific mutagenesis.<sup>84-86</sup>) The Stark spectra of these mutants exhibit a strong feature further to the red ( $\sim 930$  nm<sup>83</sup>) than for P in wild-type *Rb. sphaeroides* RCs (870 nm). This observation is consistent with the expectation that intradimer CT states should be lower in energy and therefore more strongly mixed in the heterodimer than in the homodimer. The effects of an electric field on both the absorption and fluorescence line shapes contains a wealth of information which largely remains to be understood.

Since it appears that charge-transfer states involving B are not very important in determining the properties of  $^1P$ , we return to the question of the role of B. The coupling between  $^1P$  and B required for B to be important for the initial electron-transfer reaction between  $^1P$  and H is small relative to that required to significantly affect the electronic nature and spectral properties of the special pair. The spectral properties of the chromophores in many covalently linked organic donor-acceptor complexes in which efficient electron-transfer reactions occur are unchanged as indicated by the fact that the absorption spectrum of the complex is the sum of those for the individual donor and acceptor molecules. Superexchange via the state  $P^1B$  has not previously been considered even though this state also seems likely to be important because of the physical proximity of B and P and the energetic proximity of the states  $^1B$  and  $^1P$  as indicated by the electronic absorption spectrum.

In summary, a model that is consistent with the data suggests that the moderately dipolar character of  $^1P$  is due to significant but slightly different contributions from the intradimer charge-transfer states  $P_M^{+}P_L^{-}$  and  $P_L^{+}P_M^{-}$ .<sup>59</sup> In addition, there must be some small coupling to either  $P^{+}B^{-}$  or  $^1B$  to mediate the electron transfer from P to H, but this coupling is not large enough to significantly affect the electronic nature of  $^1P$ . In the presence of an electric field, the mixing with  $^1B$  would be largely unaffected while mixing with the  $P^{+}B^{-}$  states may be affected, but if this mixing is not a major determinant of the electronic nature of  $^1P$ , the change would be too small to provide an observable first-derivative component to the absorption Stark effect spectrum. The relatively small magnitude of the effect of an electric field on the yield of fluorescence from  $^1P$ <sup>28,58</sup> and on the rate of the initial electron-transfer reaction,<sup>68,69</sup> both measured in isotropic samples, is not easily accounted for by the current quantitative formulations of the superexchange model, but this could be due to an oversimplified treatment of the dependence of FC on  $\Delta G_{et}$  rather than a problem with the basic conceptual framework.

(82) Norris, J. R. Personal communication.

(83) Hammes, S.; Mazzola, L.; Boxer, S. G.; Gaul, D.; Schenck, C. *Proc. Natl. Acad. Sci. U.S.A.*, submitted for publication.

(84) Bylina, E. J.; Youvan, D. C. *Proc. Natl. Acad. Sci. U.S.A.* **1988**, *85*, 7226-7230.

(85) Kirmaier, C.; Holten, D.; Bylina, E. J.; Youvan, D. C. *Proc. Natl. Acad. Sci. U.S.A.* **1988**, *85*, 7562-7566.

(86) Kirmaier, C.; Bylina, E. J.; Youvan, D. C.; Holten, D. *Chem. Phys. Lett.* **1989**, *159*, 251-257.

(80) Ditson, S. L.; Davis, R. C.; Pearlstein, R. M. *Biochim. Biophys. Acta* **1984**, *766*, 623-629.

(81) Hammes, S.; Boxer, S. G. Manuscript in preparation.

### Energetics of Charge Separation

#### Phosphorescence from the Triplet State of the Special Pair.

The relationship between the energetics and kinetics of the initial electron-transfer step was stressed in the previous section. In fact, it is not a simple matter to measure  $\Delta G^\circ_{et}$  in the RC. For typical electron-transfer reactions in solution,  $\Delta G^\circ_{et}$  is obtained from the redox potentials of the donor and acceptor. It is quite difficult to obtain redox potentials in the RC, especially for reduction of the initial electron acceptor I whose potential is very negative. (Most of the literature on magnetic field effects uses the notation  $P^{+}I^{-}$  for the radical pair. As discussed above, I is believed to be  $H_L$ ; nonetheless, the symbol I will be used to be consistent with the literature.) Furthermore, it is not clear that potentials obtained independently for P and I are relevant when both  $P^{+}$  and  $I^{-}$  are present or that equilibrium potentials provide an adequate description of the energetics of very short-lived states. This has led to the development of several methods for determining the energy of the  $P^{+}I^{-}$  state in situ. Woodbury and Parson have studied the temperature dependence of the delayed (recombination) fluorescence amplitude to estimate the equilibrium constant for  $^1PI \rightleftharpoons P^{+}I^{-}$ .<sup>87</sup> We have measured the free energy and enthalpy of  $P^{+}I^{-}$  relative to the triplet state of P which is formed as shown in Figure 3A when  $Q_A$  is removed.<sup>88,89</sup> The difference between the results of these two experiments may provide insight into the role of time-dependent solvation of the ion-pair intermediates by the protein environment.

Since we obtained the energy of  $P^{+}I^{-}$  relative to  $^3P$ , it is necessary to know the energy of the  $^3P$  state, a formidable task because  $^3P$  emits in the near-infrared region with a quantum yield on the order of  $10^{-7}$ . We observed the phosphorescence spectrum of RCs shown in Figure 11,<sup>90</sup> as well as the phosphorescence spectra for all of the common bacteriochlorins,<sup>91</sup> using an ultra-high sensitivity liquid nitrogen cooled germanium-photodiode detector. These data reveal that the singlet-triplet splitting for the special pair is smaller than for a monomeric bacteriochlorophyll. This is consistent with some degree of electron delocalization between the macrocycles in the  $^3P$  state. In addition to providing the energy of triplet states, which has been the subject of a great deal of speculation, these data have interesting consequences for exploring the mechanism of triplet energy transfer in the RC, a topic which closely parallels the discussion of electron-transfer mechanisms in the previous section.

Most RCs contain a carotenoid which has recently been located by X-ray crystallography to be adjacent to the monomeric  $B_M$  about 10 Å from the special pair (Figure 1).<sup>17,18</sup> The role of carotenoids in photosynthesis has been a subject of interest for many years:<sup>92</sup> the carotenoids can serve as antenna pigments transferring singlet energy if they are very close to the acceptor (their singlet lifetime is typically less than 10 ps<sup>93</sup>), and they can quench the triplet states of the photosynthetic pigments, protecting pigments whose triplet states would otherwise efficiently sensitize the formation of highly reactive singlet oxygen. Moore, Gust, and co-workers have prepared and characterized several covalently linked porphyrin-carotenoid complexes which beautifully demonstrate this combined role.<sup>94</sup> In wild-type *Rb. sphaeroides* RCs the special pair triplet state transfers its energy rapidly (nanoseconds) to the carotenoid,<sup>95</sup> whereas this transfer does not occur in *Rps. viridis* RCs.<sup>96</sup> Since triplet energy transfer occurs via

an exchange mechanism, and the special pair and the carotenoid are separated by about 10 Å, the mechanism of transfer is likely to involve the intervening  $B_M$ . In order for this mechanism to be viable, the energetics of triplet states must be appropriate. The monomeric BChl in *Rb. sphaeroides* RCs absorbs at 802 nm (Figure 6); subtracting the energy of a monomer BChl *a* Stokes shift and the singlet-triplet splitting determined for BChl *a* from the phosphorescence spectrum in a glass,<sup>91</sup> the triplet energy of the monomer BChl *a* in the RC is estimated to be within 200 cm<sup>-1</sup> of the  $^3P$  energy. Thus, we have proposed that the pathway of triplet energy transfer is likely via activated formation of the monomer BChl *a* triplet state which then transfers its energy to the carotenoid. (An activation energy of  $200 \pm 40$  cm<sup>-1</sup> for the net transfer to carotenoid has been reported.<sup>97,98</sup>) This pathway of energy transfer is not possible in *Rps. viridis* because the calculated BChl *b* monomer triplet energy is estimated to be more than 1000 cm<sup>-1</sup> above the special pair triplet energy in that species.<sup>91</sup>

It is interesting that *electron transfer* along the L side of the RC appears not to involve formation of the discrete intermediate  $P^{+}B^{-}$  as discussed in the last section, while *triplet energy transfer* from  $^3P$  to the carotenoid can be rationalized as occurring via a two-step hopping mechanism involving formation of the intermediate  $^3B_M$  in *Rb. sphaeroides*. Electron transfer and triplet energy transfer by an exchange mechanism can be viewed as arising from the same interaction.<sup>99</sup> In general, one expects parallel activated and superexchange pathways (see e.g. Figure 10). Superexchange does not appear to play a significant role in mediating triplet energy transfer in this system, in contrast to electron transfer. Although triplet energy transfer on the tens of nanoseconds time scale ensures complete trapping of  $^3P$  by the carotenoid during the microsecond  $^3P$  lifetime, a faster rate of electron transfer is required in order for  $k_{et}$  to compete with  $k_F$ , ensuring efficient charge separation.

**Energetics of Charge Separation.** In addition to recombination of the radical pair  $P^{+}I^{-}$  to the ground state, recombination to the excited triplet state of P is observed in  $Q_A$ -depleted RCs. This recombination proceeds through the triplet state of the radical pair,  $^3(P^{+}I^{-})$ , as shown in Figure 3A. The interconversion between  $^1(P^{+}I^{-})$  and  $^3(P^{+}I^{-})$  is characterized by a frequency  $\omega$ , which depends on the magnetic properties of the unpaired spins on  $P^{+}$  and  $I^{-}$ ;  $\omega$  can be manipulated by applying an external magnetic field. It is possible to alter the yield and reaction dynamics of any state whose formation or decay involves singlet-triplet mixing in the radical pair.<sup>100-102</sup>

The effect of an applied magnetic field on the relative  $^3P$  quantum yield,  $\Phi_{^3P}$ , from 0 to 135 kG in  $Q_A$ -depleted *Rb. sphaeroides* RCs is shown in Figure 12B. The large drop between 0 and 1 kG is due to the loss of the near degeneracy of the singlet and  $T_+$  and  $T_-$  states, the rise in yield between 1 and 100 kG is due to enhanced  $S-T_0$  mixing due to the difference in *g* factors of  $P^{+}$  and  $I^{-}$ , and the leveling off above 100 kG is the infinite field limit, where the yield becomes independent of field as the rate of singlet-triplet mixing exceeds the radical pair decay rates. This infinite field limit is especially important because nuclear spin polarization effects<sup>103</sup> are least important, and the values of observables (quantum yields, rates, etc.) depend only on the scheme used to model the reaction dynamics.

We noticed that the rate of  $^3P$  decay,  $k_{obs}$ , also depends on magnetic field and that the field dependence parallels the shape

(87) Woodbury, N. W.; Parson, W. W. *Biochim. Biophys. Acta* **1984**, *767*, 345-361.

(88) Chidsey, C. E. D.; Takiff, L.; Goldstein, R. A.; Boxer, S. G. *Proc. Natl. Acad. Sci. U.S.A.* **1985**, *82*, 6850-6854.

(89) Goldstein, R. A.; Takiff, L.; Boxer, S. G. *Biochim. Biophys. Acta* **1988**, *934*, 253-263.

(90) Takiff, L.; Boxer, S. G. *Biochim. Biophys. Acta* **1988**, *932*, 325-334.

(91) Takiff, L.; Boxer, S. G. *J. Am. Chem. Soc.* **1988**, *110*, 4425-4426.

(92) Cogdell, R. J.; Frank, H. A. *Biochim. Biophys. Acta* **1987**, *895*, 63-79.

(93) Wasielewski, M. R.; Kispert, L. D. *Chem. Phys. Lett.* **1986**, *128*, 238.

(94) Moore, T. A.; Gust, D.; Mathis, P.; Mialoq, J. C.; Chachaty, C.; Bennisan, R. V.; Land, E. J.; Doizi, D.; Liddel, P. A.; Lehman, W. R.; Nemuth, G. A.; Moore, A. L. *Nature* **1984**, *307*, 630.

(95) Parson, W. W.; Monger, T. G. *Brookhaven Symp. Biol.* **1977**, *No. 28*, 195-212.

(96) Holten, D.; Windsor, M. W.; Parson, W. W.; Thornber, J. P. *Biochim. Biophys. Acta* **1978**, *501*, 112-126.

(97) Schenck, C. C.; Mathis, P.; Lutz, M. *Photochem. Photobiol.* **1984**, *39*, 407-417.

(98) Frank, H. A.; Michinicki, J.; Friesner, R. *Photochem. Photobiol.* **1983**, *38*, 451-455.

(99) Closs, G. L.; Piotrowiak, P.; MacInnis, J. M.; Fleming, G. R. *J. Am. Chem. Soc.* **1988**, *110*, 2652-2653.

(100) Hoff, A. J. *Photochem. Photobiol.* **1986**, *43*, 727-745.

(101) Boxer, S. G.; Chidsey, C. E. D.; Roelofs, M. G. *Annu. Rev. Phys. Chem.* **1983**, *34*, 389-417.

(102) Chidsey, C. E. D.; Kirmaier, C.; Holten, D.; Boxer, S. G. *Biochim. Biophys. Acta* **1984**, *766*, 424-437.

(103) Goldstein, R. A.; Boxer, S. G. *Biochem. J.* **1987**, *51*, 937-946.

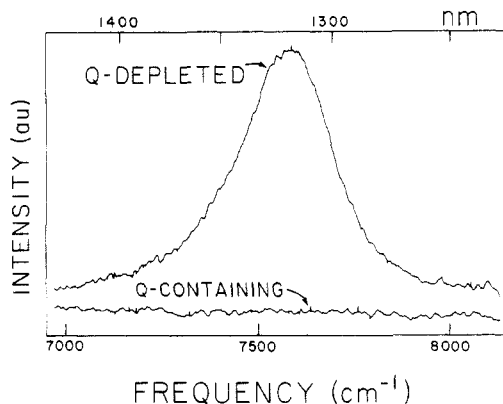


**Figure 11.** Phosphorescence spectrum of  $Q_A$ -depleted *Rb. sphaeroides* reaction centers in a PVA film at 20 K compared with that of a comparably concentrated  $Q_A$ -containing reaction center film taken under identical conditions. The  $^3P$  state is not formed in  $Q_A$ -containing RCs.

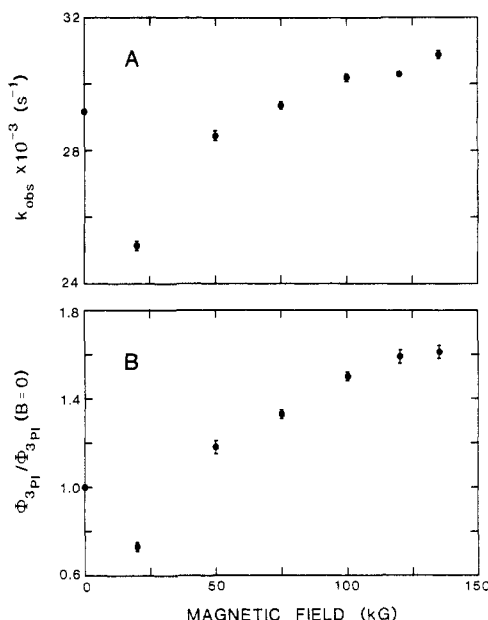


**Figure 12.** Dependence of (A)  $k_{obs}$  and (B)  $\Phi_{3PI}/\Phi_{3PI}(B=0)$  on magnetic field between 0 and 135 kG at 15 °C for quinone-depleted RCs in aqueous buffer, with probe beam polarized at the magic angle with respect to the applied magnetic field.  $k_{obs}$  is the observed rate of  $^3PI$  decay,  $\Phi_{3PI}$  is the quantum yield of  $^3PI$  formation, and  $\Phi_{3PI}(B=0)$  is the  $^3PI$  quantum yield at zero applied field.

of  $\Phi_{3P}$  (Figure 12A). Such a field dependence led us to postulate that, in addition to simple intersystem crossing,  $^3P$  can also decay to the ground state via activated reformation of  $^3(P^{*+}I^{-})$ , followed by singlet-triplet mixing and  $k_S$ . This model provides a simple explanation for the temperature dependence of  $k_{obs}$  and predicts that  $k_{obs}$  will be independent of magnetic field at lower temperatures, where decay is entirely via intersystem crossing as is observed.<sup>88</sup> The theoretical treatment of the magnetic field and temperature dependence of  $k_{obs}$  is not trivial, yet yields the following simple expression:

$$k_{obs} = k_{isc} + \frac{1}{3}k_S\Phi_{3P} \exp(-\Delta G^{\circ}_{3(P^{*+}I^{-}) \rightarrow ^3PI} / k_B T) \quad (7)$$

where  $k_B$  is the Boltzmann constant and  $T$  is temperature. Equation 7 provides two independent methods for obtaining the  $^3(P^{*+}I^{-}) \rightarrow ^3PI$  energy difference. If  $k_{obs}$  as a function of relative  $^3P$  quantum yield is fit to a straight line, the  $y$  intercept is equal to  $k_{isc}$ , while the slope is  $(1/3)k_S\Phi_{3P}(B=0) \times \exp(-\Delta G^{\circ}_{3(P^{*+}I^{-}) \rightarrow ^3PI} / k_B T)$ , where  $\Phi_{3P}(B=0)$  is the quantum yield of  $^3P$  at zero applied field.  $k_S$  and  $\Phi_{3PI}(B=0)$  have been measured previously;<sup>102</sup> substitution gives  $\Delta G^{\circ}_{3(P^{*+}I^{-}) \rightarrow ^3PI} = 1370 \pm 30 \text{ cm}^{-1}$ . Alternatively, eq 7 can be rewritten as an Arrhenius-type expression, so that  $\Delta H^{\circ}$  can be obtained from the temperature

dependence of  $k_{obs}$ . Such an analysis yields  $\Delta H^{\circ}_{3(P^{*+}I^{-}) \rightarrow ^3PI} = 1450 \pm 70 \text{ cm}^{-1}$ ; the near equivalence of  $\Delta H^{\circ}$  and  $\Delta G^{\circ}$  suggests that there is little entropy change during thermal reformation of the radical pair from  $^3P$ .

The energy of the singlet excited state is known accurately from an analysis of the absorption and fluorescence spectrum,<sup>104</sup> and the energy of  $^3P$  is known from the phosphorescence spectrum<sup>90</sup> discussed above. Combining  $\Delta G^{\circ}_{3(P^{*+}I^{-}) \rightarrow ^3PI}$  from the magnetic field effect studies and the  $^1P$  energy, we obtain  $\Delta G^{\circ}_{et} = 2120 \text{ cm}^{-1}$  (0.263 eV) at room temperature.<sup>89</sup> The energetics of all states characterized thus far in *Rb. sphaeroides* RCs are summarized in Figure 13 (see below). Because the phosphorescence maximum is approximately independent of temperature,  $\Delta G^{\circ}_{et} \sim \Delta H^{\circ}_{et}$ , and we conclude that  $\Delta G^{\circ}_{et}$  does not depend strongly on temperature. These results differ from those obtained by Woodbury and Parson using delayed fluorescence, who found that  $\Delta G^{\circ}_{et} = 0.17 \text{ eV}$  at room temperature and was strongly temperature dependent, decreasing to 0.05 eV at 100 K.<sup>87</sup> The delayed fluorescence data show a complex temperature dependence which has not been explained. The discrepancy in the room-temperature value of  $\Delta G^{\circ}_{et}$  between the energetics obtained on a nanosecond time scale by delayed fluorescence and those obtained on a longer time scale by analysis of the triplet decay may be the result of a lowering of the redox energy of  $P^{*+}I^{-}$  over a period of nanoseconds as the ion pair relaxes in its surroundings.<sup>87,104,105</sup>

In order to explore this further, we have recently extended the delayed fluorescence measurements to very high magnetic fields.<sup>106</sup> At very high magnetic fields the contribution of the  $g$ -factor difference to the singlet-triplet mixing dominates that due to the distribution of hyperfine fields in the radical pair. As a result, the concentration of  $^1(P^{*+}I^{-})$  is expected to oscillate at the frequency  $\Delta g\beta B$ , where  $B$  is the applied magnetic field strength, and the delayed fluorescence, which samples only the concentration of  $^1(P^{*+}I^{-})$ , is expected to oscillate.<sup>63</sup> Such chemical quantum beats were recently observed in a much simpler system in solution.<sup>107</sup> We did not find any evidence for the expected beats in the delayed fluorescence from RCs but instead observed a monotonic decrease in the lifetime of the magnetic-field-dependent component as the field was increased. This dependence parallels that for the triplet quantum yield and  $k_{obs}$  shown in Figure 12 and saturates above about 100 kG. From a quantitative analysis of the field dependence of the delayed fluorescence, we directly obtain the value of  $k_T = 4 \times 10^8 \text{ s}^{-1}$ .<sup>106</sup>

The absence of quantum beats in the delayed fluorescence suggests that the scheme in Figure 3A is incomplete. A key assumption leading to the prediction of delayed fluorescence quantum beats at high magnetic field is that the radical pair state which undergoes singlet-triplet mixing is formed on a time scale which is rapid compared with the singlet-triplet mixing time. (This will be true for the mechanism in Figure 3A where  $P^{*+}I^{-}$  is formed in a few picoseconds.) In the model described by Woodbury and Parson<sup>87,104</sup> to explain the multiple components of delayed fluorescence, the radical pair is initially formed in an unrelaxed nuclear coordinate state, and the relaxation occurs on a nanosecond time scale, so that the initiation of singlet-triplet mixing in  $^1(P^{*+}I^{-})$  should occur over a distribution of times. Such a distribution would spread the times of initiation of singlet-triplet mixing in  $P^{*+}I^{-}$ , and no delayed fluorescence quantum beats would then be expected at very high magnetic field.<sup>106</sup> Independent of this observation, it can be shown that some intermediate state is needed between  $^1P$  and  $^1(P^{*+}I^{-})$  in Figure 3A in order to explain the magnitude of the magnetic field effect on  $\Phi_{3PI}$  shown in Figure 12B.<sup>108</sup> Since the intermediacy of a state such as  $P^{*+}B^{-}$  with

(104) Woodbury, N. W.; Parson, W. W. *Biochim. Biophys. Acta* **1986**, 850, 197–210.

(105) Woodbury, N. W.; Parson, W. W.; Gunner, M. R.; Prince, R. C.; Dutton, P. L. *Biochim. Biophys. Acta* **1986**, 851, 6–22.

(106) Goldstein, R. A.; Boxer, S. G. *Biochim. Biophys. Acta* **1989**, 977, 70–77.

(107) Veselov, A. V.; Melekhov, V. I.; Anisimov, O. A.; Molin, Yu. N. *Chem. Phys. Lett.* **1987**, 136, 263–266.

(108) Goldstein, R. A.; Boxer, S. G. *Biochim. Biophys. Acta* **1989**, 977, 78–86.

a lifetime of nanoseconds has been ruled out by the transient absorption and electric field effect measurements described earlier, we come back to the proposal of Woodbury and Parson<sup>87,104</sup> that the intermediate is an unrelaxed form of  $P^{+}I^{-}$ .

Finally, we return to the central question: what are the appropriate energetics to describe the initial electron-transfer step? We suggest that the results shown in Figure 13 obtained on the microsecond time scale are indicative of the equilibrium energetics of states in the RC. However, the energetics which are relevant for the initial charge separation may be better characterized by the delayed fluorescence results of Woodbury and Parson.<sup>87</sup> The nature of the unrelaxed state remains open: it could involve solvation by the protein or motions within the reactive components such as P. The role of coupling to medium modes has been discussed for electron transfer in photosynthetic systems.<sup>62</sup> The dilemma posed by comparisons of electron-transfer energetics on different time scales indicates that these issues are also important for understanding the initial steps in photosynthesis. Furthermore, the appropriate time scale can be shifted by changing the temperature or viscosity; consequently, the dependence of observables on these experimental variables may not be simple to interpret.<sup>8,12</sup>

**Relationship of Electron Transfer in RCs to Other Proteins.** The issues of time-dependent coupling to the matrix and temperature-dependent energetics are important, as they relate to the possible role of the protein in tuning the redox potential of intermediates and to the magnitude of the outer sphere (solvent) reorganization energy. Because the initial charge separation reaction is apparently activationless,<sup>8,12</sup> its driving force should be approximately equal to the reorganization energy.<sup>61</sup> The reorganization energy in conventional treatments is determined by changes in the vibrational frequencies between reactants and products and changes in the organization of the solvent when charge is separated or recombined. For electron transfer in the RC, the reactants and products are large aromatic molecules with extended  $\pi$ -systems, so relatively small changes in bond lengths are expected upon formation of  $\pi$ -cation or  $\pi$ -anion radicals. The solvent is primarily the RC protein, consisting largely of nonpolar, though polarizable, residues. Relatively little information is available on reorganization energies or solvation dynamics in proteins. It has been suggested that fairly large reorganization energies (1–2 eV) are a general characteristic of electron-transfer reactions occurring in proteins.<sup>109</sup>

Unfortunately, generalizations of the type discussed above consistently ignore electron transfer in the RC, even though this is the only system studied in detail whose native function is electron transfer. Each of the following electron-transfer reactions in the RC is found to be approximately independent of temperature:  $^1P \rightarrow P^{+}I^{-}$ , discussed in detail above;<sup>12</sup>  $^3(P^{+}I^{-}) \rightarrow ^3P$ ;<sup>110</sup>  $P^{+}I^{-} \rightarrow P^{+}IQ_A^{-}$ ,<sup>8</sup> and  $P^{+}Q_A^{-} \rightarrow PQ_A$ .<sup>16</sup> As seen in Figure 13,  $\Delta G^{\circ}$  for each of these reactions is quite different. Electron-transfer reactions are expected to be activationless (temperature independent) when they are optimally exothermic, i.e., when  $\Delta G^{\circ}_{et}$  is about equal to the total reorganization energy. This has led to the suggestion<sup>62</sup> that, for the forward reactions, the nature of the reactants and the protein has evolved to achieve this delicate balance of rate and driving force leading to the fastest rates for the smallest  $\Delta G^{\circ}$ , thereby storing the largest share of the initial photon energy. It is possible that the reorganization energy is smaller than expected for these electron-transfer reactions because the protein (solvent) has evolved so that the environment of the chromophores is already in a configuration that is compatible with the charge-separated states even prior to their formation. For such a configuration only a small reorganization of the protein would accompany electron transfer. This possibility exists for reactions in a protein, but not in fluid solution, because of the constraints on the positions of polar and polarizable groups imposed by the protein secondary and tertiary structure. Thus, the ar-

gument that the reorganization energy in proteins is always large appears not to apply to the photosynthetic RC. In fact, it seems most reasonable that proteins whose native function is electron transfer evolve in order to optimize whatever rate and free energy combination is best suited to their function (obviously this need not be the fastest rate).

**Summary and Problems for the Future.** As outlined in this paper, considerable experimental progress has been made in understanding the nature of the early events in bacterial photosynthesis. Both the hole-burning and absorption Stark effect experiments suggest that the excited electronic state of the special pair which initiates photosynthesis is quite different from that of a typical aromatic molecule. Subpicosecond kinetics and the fluorescence electric field effect data suggest that long-distance electron transfer between the excited state of the special pair and the bacteriopheophytin electron acceptor does not involve populating the state  $P^{+}B^{-}$  as a real intermediate; rather, B appears to play some role in mediating the coupling between  $^1PH$  and  $P^{+}H^{-}$ , either via the  $P^{+}B^{-}$  state as has been widely discussed<sup>20,72–74,76,77</sup> or via a relatively neutral state such as  $P^1B$ .

We conclude with a brief discussion of unresolved issues and directions for the future. Although the data lead to the notion that superexchange is the key to understanding the initial electron-transfer step, there are problems with this proposal, especially those noted by Marcus;<sup>78,79</sup> alternative models have been suggested by Fischer and Scherer.<sup>111,112</sup> What is missing is direct experimental information on the energetics and potential surfaces of states such as  $P^{+}P^{-}$  and  $P^{+}B^{-}$ . An alternative approach is to calculate the energies of states by a complete simulation of the electrostatic environment around putative intermediates. A first attempt in this direction has recently been presented.<sup>50,113</sup>

(111) Fischer, S. F.; Scherer, P. O. *J. Chem. Phys. Lett.* **1987**, *115*, 151–158.

(112) Scherer, P. O. J.; Fischer, S. F. *Chem. Phys. Lett.* **1987**, *141*, 179–185.

(113) Creighton, S.; Hwang, J.-K.; Warshel, A.; Parson, W. W.; Norris, J. *Biochemistry* **1988**, *27*, 774–781.

(114) Chen, F. P.; Hanson, D. M.; Fox, D. *J. Chem. Phys.* **1975**, *63*, 3878–3885.

(115) Bagchi, B.; Oxtoby, D. W.; Fleming, G. R. *Chem. Phys.* **1984**, *86*, 257–267.

(116) Budil, D. E.; Gast, P.; Chang, C.-H.; Schiffer, M.; Norris, J. R. *Annu. Rev. Phys. Chem.* **1987**, *38*, 561–583.

(117) This local field correction,  $F_{int} = fF_{ext}$ , has been considered in detail elsewhere.<sup>114</sup> In a complex inhomogeneous dielectric such as the RC protein, the value of  $f$  may vary from site to site, and this may have significant functional consequences. The value of  $f$  is expected to be on the order of 1.2–1.5 for a dielectric constant of 2. In general, the local field correction is a tensor quantity. If the local field correction is very anisotropic in the RC, this introduces some uncertainty into the evaluation of  $\zeta_A$  and  $\zeta_{et}$ .

(118) Since the Stark effect measures the change in dipole moment, it is possible that the excited-state moment is actually smaller than the ground-state moment. Even if the excited-state moment is larger than the ground-state moment, the ground-state moment could be substantial, as suggested by some calculations [Plato, M., personal communication]. At the present time, there is no obvious way to obtain experimental information on the electric dipole moment of the special pair neutral ground state; this remains a major uncertainty in the interpretation of magnitude and direction information in all Stark effect measurements on the RC.

(119) In fluid solution, a large and time-dependent Stokes shift is often indicative of a fluorescent state which is more dipolar than the ground state.<sup>115</sup> The Stokes shift for the special pair in the RC is larger than for a typical chlorophyll-type molecule, but the stimulated emission line shape appears not to change during the lifetime of  $^1P$  [Parson, W. W., personal communication]. However, because the initial electron-transfer reaction is so fast ( $k_{et} \sim 3 \times 10^{11} \text{ s}^{-1}$ ), solvation by the amino acid residues in the hydrophobic interior of the RC may not have sufficient time to occur. In other words, the observed Stokes shift for the special pair in the RC may not be indicative of the equilibrium properties of the emitting state because of the relative time scales of electron transfer and solvation by the protein environment.

(120) Lockhart, D. J. Ph.D. Thesis, Stanford University, 1989.

(121) There is no evidence in the absorption Stark effect of P (Figure 6) that its oscillator strength is field dependent.

(122) If the charge distribution in  $P^{+}$  is not symmetrical on the few picosecond time scale, the use of the geometric center of P may not be appropriate; however, nothing is known about the charge distribution on this time scale. If charge asymmetry in  $P^{+}$  is included in a calculation of the direction of  $\Delta\mu_{et}$ , then it is essential that charge asymmetry in  $^1P$  also be included because  $\Delta\mu_{et} = \mu(P^{+}I^{-}) - \mu(^1P)$ . If the charge asymmetries in  $^1P$  and  $P^{+}$  are comparable (cf. ref 70), then these asymmetries largely cancel, and the use of the geometric center of P is a reasonable approximation.

(109) Conklin, K. T.; McLendon, G. *J. Am. Chem. Soc.* **1988**, *110*, 3345–3350.

(110) Ogorodnik, A.; Remy-Richter, N.; Michel-Beyerle, M. E.; Feick, R. *Chem. Phys. Lett.* **1987**, *135*, 576.



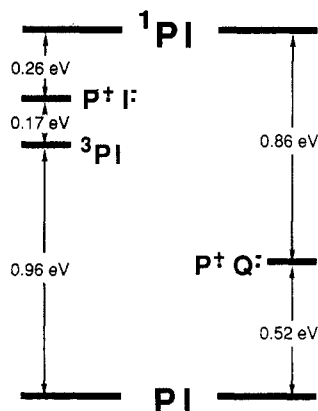


**Figure 13.** Summary of energetics in *Rb. sphaeroides* RCs obtained from analysis of the decay of the  $^3P$  state. As discussed in the text, these are likely to be close to the equilibrium energies and may not reflect the energetics on a very short time scale which may be important for the initial charge separation step (cf. ref 104 and 105).

However, energetics alone will not suffice; the shapes and displacements of potential surfaces as well as an accurate calculation of the electronic coupling are also required. The subtlety of the problem is reflected in the question of the origin of unidirectional

electron transfer along the L-side of the RC, illustrated in Figure 1. As pointed out in the analysis of Michel-Beyerle et al.,<sup>20</sup> it appears that slight differences in distances on the M- and L-sides and differential electrostatic stabilization due to the protein environment combine to produce unidirectional electron transfer, although this remains an open question. This subject can now be approached by recombinant DNA methods<sup>82-86</sup> and by measurements of electric field effects on reaction rates and pathways.

*Note Added in Proof.* Zinth and co-workers have recently published time-resolved kinetic data which purport to show a two-step formation of  $P^+BPheo^-$  in *Rb. sphaeroides* RCs at room temperature [Holzapfel, W.; Finkle, U.; Kaiser, W.; Oesterhelt, D.; Scheer, H.; Stolz, H. U.; Zinth, W. *Chem. Phys. Lett.* **1989**, *160*, 1-7]. This result differs from earlier quantitative analyses of the kinetics [cf. ref 12 and 13] and the electric field induced fluorescence anisotropy [cf. ref 28] at low temperature. Thus, the mechanism of the initial charge separation step is far from settled.

*Acknowledgment.* Parts of this work were supported by grants from the NSF Biophysics Program and a Presidential Young Investigator Award to S.G.B. We thank Drs. Bixon, Holten, Jortner, Parson, and Small for providing manuscripts prior to publication and Drs. Bixon, Fischer, Friesner, Holten, Jortner, Marcus, Norris, Parson, Plato, Ulstrup, and Woodbury for helpful discussions.

## ARTICLES

### Experimental Design Optimization and Confidence Interval Estimation in Multieponential NMR Relaxation Measurements

John D. Decatur and Thomas C. Farrar\*

Department of Chemistry, University of Wisconsin, Madison, Wisconsin 53706 (Received: April 3, 1989)

Numerical simulations were used to estimate the precision of parameters responsible for NMR spin-lattice relaxation in a coupled two-spin system where two relaxation mechanisms, dipole-dipole and chemical shift anisotropy, are present. Parameter confidence intervals in nonlinear least-squares fitting, necessary for multiexponential relaxation, can be obtained without restrictive assumptions. The simulations allow one to investigate the effect of experimental variables on parameter precision without performing many lengthy experiments. It was found that the results of several pulse experiments, including the traditional inversion recovery, must be fit simultaneously to achieve reasonable precision. Precision depends upon many factors including the nucleus observed, how the recovery curves are sampled, the sample temperature stability, and the number of simultaneously estimated parameters.

#### Introduction

Measurement of spin-lattice relaxation times is a powerful method for obtaining information about the structure and dynamics of molecules in solution. If the relaxation is due to a single relaxation mechanism, the inversion recovery curve for either a coupled or decoupled spin system can usually be characterized, to a high degree of approximation, by a single-exponential time constant,  $T_1$ .<sup>1</sup> When two or more relaxation processes are present, recovery curves may be multiexponential.<sup>2,3</sup> At the high fields

commonly used, the contribution to relaxation from the chemical shift anisotropy (CSA) may be as large as or even exceed the dipolar contribution. For  $PHO_3^{2-}$  at 4.7 T (200 MHz  $^1H$ ), interference terms between dipolar and CSA relaxation cause very noticeable effects in both the observed spectrum and in the inversion recovery curves. Previous work in this laboratory has demonstrated that these effects can be exploited to yield a simultaneous determination of all molecular parameters responsible for nuclear spin-relaxation.<sup>4</sup> For  $PHO_3^{2-}$ , these include the chemical shift anisotropy of the proton and the phosphorus, the H-P bond distance, and the molecular correlation time.

(1) Campbell, I. D.; Freeman, R. J. *Magn. Reson.* **1973**, *11*, 143-162.

(2) Shimizu, H. J. *Chem. Phys.* **1964**, *40*(11), 3357-3364.

(3) Mackor, E. L.; MacLean, C. *Prog. Nucl. Magn. Reson. Spectrosc.* **1967**, *3*, 129-157.

(4) Farrar, T. C.; Locker, I. C. *J. Chem. Phys.* **1987**, *87*(6), 3281-3287. See also: *Z. Phys. Chem. (Munich)* **1987**, *151*, 25-33.